Journal of Soil Science and Plant Nutrition
https://doi.org/10.1007/s42729-022-00983-w

ORIGINAL PAPER

Exogenous Coumarin Decreases Phytotoxic Effects of Manganese by Regulating Ascorbate–Glutathione Cycle and Glyoxalase System to Improve Photosynthesis and Nutrient Acquisition in Sesame (*Sesamum indicum* L.)

Mudassir Iqbal Shad[1] · Muhammad Arslan Ashraf[1] · Rizwan Rasheed[1] · Iqbal Hussain[1] · Shafaqat Ali[2,3]

Received: 23 March 2022 / Accepted: 22 August 2022

Abstract
Coumarin (COU) is an essential phenolic compound safeguarding plants under environmental constraints. Coumarin-induced salinity tolerance is reported in tomato, wheat and sorghum. However, the underlying mechanism by which COU mediates stress tolerance is not established, particularly under manganese (Mn) toxicity. Therefore, the present study was undertaken to examine COU-mediated regulation of Mn tolerance mechanism in sesame. Plants were subjected to two Mn levels (450 and 750 mg kg^{-1}), given as $MnSO_4$. Sesame seeds were primed in different doses of COU (0, 50, 100, and 150 mg L^{-1}). Coumarin effects on photosynthesis, SPAD values, glyoxalase system, osmolyte accumulation, secondary metabolism, ROS generation and detoxification, ascorbate–glutathione cycle and ions homeostasis were studied in sesame. Our results manifested a notable drop in growth, chlorophyll contents, leaf relative water content, photosynthesis, and nutrient acquisition in plants under Mn toxicity. Further, excess Mn substantially increased oxidative damage mirrored as higher endogenous levels of hydrogen peroxide (H_2O_2), superoxide radical ($O_2^{\bullet-}$), malondialdehyde, and electrolyte leakage. Coumarin protected plants from oxidative injury by strengthening the activities of ascorbate–glutathione cycle enzymes under Mn toxicity. Histochemical studies revealed lesser H_2O_2 and $O_2^{\bullet-}$ generation in plants administered COU under Mn toxicity. Besides, COU brought a significant fall in the methylglyoxal levels by increasing the activities of glyoxalase enzymes. Moreover, proline and glycine betaine accumulation were several folds greater in plants pre-treated with COU under Mn toxicity. Coumarin lessened chlorophyll degradation, bettered photosynthesis, and abridged oxidative injury that might have enhanced tolerance to Mn toxicity.

Keywords Metal toxicity · Ions homeostasis · Oxidative injury · Lipid peroxidation · ROS generation · Membrane integrity · Oxidative defense · Osmolyte accumulation

1 Introduction

Manganese (Mn) mediates plant growth and development due to its role as an essential micronutrient in crucial cellular metabolic activities. Notably, Mn is a vital part of structural proteins and plays an important role in photosynthesis (Alejandro et al. 2020). Contrariwise, excess Mn levels in the soil become toxic for plant survival and are considered a significant constraint for plant growth and productivity, especially in acidic soils (Liu et al. 2020; Noor et al. 2022). Soil acidity occurs due to extended usage of land that decreases soil pH. Acidic soils contain abundant hydrogen ions (H^+), which dissolve mineral Mn oxides to increase Mn availability in

✉ Muhammad Arslan Ashraf
arsilpk@gmail.com; marslanashraf@gcuf.edu.pk

[1] Department of Botany, Government College University Faisalabad, Faisalabad 38000, Pakistan

[2] Department of Environmental Sciences and Engineering, Government College University Faisalabad, Faisalabad 38000, Pakistan

[3] Department of Biological Sciences and Technology, China Medical University, Taichung 40402, Taiwan

Published online: 06 September 2022

soil. Consequently, plants encounter Mn toxicity due to the release of surplus Mn ions (Mn^{2+}) in the soil (Noor et al. 2022). The availability of electrons is greater in acidic soils with organic amendments, which enhance Mn availability and create Mn toxicity in plants. Mn toxicity reduces photosynthetic rate, impedes chlorophyll biosynthesis, and promotes the buildup of oxidized Mn in the leaf apoplast (Socha and Guerinot 2014). As a result, brown patches on mature leaves appear as interveinal chlorosis and tissue necrosis, which are common signs of Mn toxicity. Mn toxicity abridges yield quality and production in crops (Noor et al. 2022).

The accumulation of Mn is not confined to a single organelle, as is the case with other heavy metals (chromium, Cr; copper, Cu; cadmium, Cd; aluminum, Al; and nickel, Ni), and plant species show remarkable variations concerning the storage sites of Mn (Papadakis et al. 2007). For instance, chloroplasts are among the primary locations for Mn accumulation, which is the reason for inhibited photosynthesis under Mn toxicity. Concurrently, Mn may replace Mg in chlorophyll molecules or link to the thylakoid matrix, damaging the chloroplast ultrastructure (Costa et al. 2017). Noor et al. (2022) also documented fall in photosynthesis as the first response of plants to Mn toxicity. Likewise, Li et al. (2010) reported abridging in chlorophyll contents and photosynthesis efficiency in plants under Mn toxicity. Consequently, photo-oxidation of chlorophyll molecules induces Mn oxidation in the chloroplast, generating reactive oxygen species (ROS). Excessive ROS levels severely impair chlorophyll molecules and chloroplast ultrastructure. Further, hydrogen peroxide (H_2O_2) and superoxide radicals ($O_2^{\bullet-}$) among ROS are more lethal due to their potential to interact with nucleic acid, proteins, lipids, and pigments, thereby hampering metabolic activities and cell membrane integrity in plants under Mn toxicity (Noor et al. 2022). Manganese toxicity inhibits the uptake and translocation of essential plant nutrients such as P, Ca, Fe, and Mg due to resemblance in ligand binding ability and ionic radius (Millaleo et al. 2013). Toxic Mn levels vary significantly with plant species and genotypes. Plants disperse excess Mn levels to vacuoles, cell walls, and various leaf tissues (Alejandro et al. 2020).

Plants undertake several approaches to tolerate excess Mn stress, including compartmentalization and sequestration of Mn, restricted Mn uptake and translocation, homogenous dispersion of excess Mn to various leaf tissues, and strengthened antioxidant system to scavenge ROS (Santos et al. 2017; Li et al. 2019; Kumari et al. 2022; Skórka et al. 2022). Besides, the execution of these strategies relies entirely on plant species (Faria et al. 2020). The activation of antioxidant defense machinery is the essential safeguard against oxidative damage due to metalloid toxicity (Demidchik 2015; Qureshi et al. 2020). Superoxide dismutase (SOD) significantly circumvents oxidative damage because it is the sole enzyme in the detoxification of $O_2^{\bullet-}$ to H_2O_2 and O_2 (Hasanuzzaman et al. 2020). Catalase (CAT) and peroxidase (POD) enzymes effectively detoxify H_2O_2 (Ashraf et al. 2021). The other metabolic pathway that detoxifies H_2O_2 is ascorbate–glutathione cycle. The enzymes of this cycle are present in peroxisomes, chloroplasts, mitochondria, and cytosol. The enzymes of ASA-GSH cycle, namely glutathione reductase (GR), dehydroascorbate reductase (DHAR), monodehydroascorbate reductase (MDHAR), and ascorbate peroxidase (APX), subside oxidative damage by maintaining the cellular glutathione and ascorbate pool. Additionally, glutathione and ascorbate are essential non-enzymatic antioxidant compounds that generate metallothioneins and phytochelatins, the primary detoxification compounds for heavy metals (Kaya et al. 2020). Furthermore, glutathione *S*-transferase (GST) is an essential ROS-detoxification enzyme that also does xenobiotic detoxification (Hasanuzzaman et al. 2019). Methylglyoxal (MG) is a highly reactive and toxic compound widely studied in animals, while its role in most plants remains unknown. Several studies exhibit the overproduction of MG in plants under abiotic stress (Hasanuzzaman et al. 2017). The glyoxalase system includes glyoxalase enzymes I and II (Gly I and Gly II) alongside GSH compounds that act together to offset MG effects by converting it into safe compounds (Hasanuzzaman et al. 2011, 2018b).

Coumarin (COU), a hydroxycinnamic phenolic acid, is a phenolic compound with considerable antioxidant potential, antimicrobial activity, and a well-established plant growth promoter (Saleh et al. 2015). Coumarin regulates critical physiological processes in a dose-dependent manner at different growth stages (Parvin et al. 2021). In this context, Saleh et al. (2015) reported COU-mediated accumulation of antioxidant compounds that resulted in bettered salinity tolerance in wheat. Likewise, Parvin et al. (2021) also documented COU-induced better salinity tolerance in tomato plants. However, there exists no information to date on COU-mediated regulation of photosynthesis, oxidative defense, glyoxalase system, and nutrient acquisition in plants under Mn toxicity. Consequently, the present study was undertaken to evaluate the effects of COU on the glyoxalase system, antioxidant response, osmolyte accumulation, generation of oxidative stress markers, ions homeostasis, nitric oxide, and hydrogen sulphide levels in sesame plants under Mn toxicity. Sesame is an essential oil crop distributed around the globe with broad prospects for the phytoremediation of metal contaminated soils due to their high metal accumulation capacity and high biomass (Zhou et al. 2020).

2 Materials and methods

2.1 Plant material

Sesame (*Sesamum indicum* L.) seeds of cultivar TS5 were procured from Ayub Agricultural research institute Faisalabad, Pakistan. Seeds were surface sterilized with sodium hypochlorite (1%) for 5 min followed by thorough washing with distilled water.

2.2 Experimental plan and treatment details

Surface sterilized seeds were sown in pots filled with soil spiked with 450 and 750 mg kg^{-1} Mn, given as $MnSO_4$. Manganese levels are selected based on our preliminary experimental studies (Figure S1 & S2; Appendix-I). Two weeks after germination, thinning was done to keep one plant in each pot. The physiochemical properties of soil were as; sandy loam soil, ECe 2.61 dS m^{-1}, pH 6.1, organic matter 0.44%, SAR 5.51 $mmol^{-1}$, HCO_3^- 3.58 mmol L^{-1}, available P 2.01 mg kg^{-1}, SO_4^{2-} 5.98 mmol L^{-1}, Cl^- 2.05 mmol L^{-1}, K^+ 0.07 mmol L^{-1}, and Na^+ 3.75 mmol L^{-1}. Soil physiochemical analysis was performed following the method of Habiba et al. (2019). Coumarin levels were obtained from pre-experimental studies (Figure S3 & S4; Appendix-II). Sesame seeds were primed in deionized water and various coumarin concentrations (50, 100 and 150 mg L^{-1}) for 24 h. Primed seeds were sown in plastic pots filled with soil spiked with Mn (450 and 750 mg kg^{-1} soil). Research design was completely randomized design with factorial arrangement, and there were four replicates of each treatment. Plants were supplemented with urea, potassium sulfate and diammonium phosphate as source of potassium (K), nitrogen (N) and phosphorus (P), respectively. Fertilizers were applied at rate of 25, 120, and 50 kg ha^{-1} (K, N and P, respectively) (Habiba et al. 2019). After 60 days of germination, plants were harvested and various growth, physiological and biochemical attributes were recorded. The experiment had the following treatments:

(i) Unprimed + 0 Mn
(ii) Hydroprimed + 0 Mn
(iii) COU 50 mg L^{-1} primed + 0 Mn
(iv) COU 100 mg L^{-1} primed + 0 Mn
(v) COU 150 mg L^{-1} primed + 0 Mn
(vi) Unprimed + 450 Mn
(vii) Hydroprimed + 450 Mn
(viii) COU 50 mg L^{-1} primed + 450 Mn
(ix) COU 100 mg L^{-1} primed + 450 Mn
(x) COU 150 mg L^{-1} primed + 450 Mn
(xi) Unprimed + 750 Mn
(xii) Hydroprimed + 750 Mn
(xiii) COU 50 mg L^{-1} primed + 750 Mn
(xiv) COU 100 mg L^{-1} primed + 750 Mn
(xv) COU 150 mg L^{-1} primed + 750 Mn

2.3 Growth characteristics

Plants were harvested and shoot and root fresh and dry biomass, leaf area and relative water content (LRWC) were recorded. Leaf area was calculated following the equation (Leaf area = leaf length × leaf width × 0.75) of Gardner et al. (1985). LRWC was measured using method of Barrs and Weatherley (1962) and calculated using following equation.

LRWC (%) = (fresh weight -dry weight)/ (turgid weight—dry weight) × 100.

2.4 Leaf pigments, SPAD values and gas exchange characteristics

Photosynthetic pigments (Chlorophyll *a*, *b*, total chlorophyll and carotenoids) were estimated via the methodology of Lichtenthaler (1987). Fresh leaf tissue (0.5) g was ground in 80% methanol solution (10 mL). The optical density (OD) was observed at 470, 646.8 and 663.2 nm using spectrophotometer. β-cyanin and β-xanthine were estimated from fresh leaf tissue using 80% methanol and 50 mM ascorbic acid (Sarker and Oba 2018). The OD was recorded at 540 and 475 nm with spectrophotometer. β-carotene was determined via homogenizing fresh leaf tissue (0.5 g) in 10 mL of 80% methanol. Homogenate was centrifuged and supernatant was used to record OD at 510 and 480 nm (Jensen 1978). SPAD values were taken using a SPAD meter (Hansatech instruments, model CL-01). Stomatal conductance, transpiration rate, water use efficiency and net photosynthesis rate were estimated (Li-COR Lincoln, USA).

2.5 Malondialdehyde *(MDA)*

Fresh leaf tissue (0.5 g) was homogenized in 10 mL of 6% trichloroacetic acid (TCA) solution. The supernatant (0.5 mL) was allowed to react with 5% thiobarbituric acid (TBA) followed by incubation at 95 °C for 35 min. The OD was recorded at 532 and 600 nm using a spectrophotometer (Cakmak and Horst 1991).

2.6 Hydrogen peroxide (H_2O_2)

The supernatant (0.5 mL) from 6% TCA grinding of fresh leaf material (0.5) was added to 0.5 mL potassium phosphate buffer (50 mM; pH 7.8). The reaction solution was incubated for 30 min at room temperature before taking OD at 390 nm (Velikova et al. 2000).

2.7 Superoxide radical ($O_2^{\bullet-}$)

The biosynthesis of $O_2^{\bullet-}$ was measured following the technique of Yang et al. (2011). Fresh leaf tissue (0.5 g) was finely ground and mixed with hydroxylamine hydrochloride. Then the mixture was incubated for 30 min at room temperature. Further, 7 mM naphthylamine and sulfanilamide (17 mM) were added to the reaction mixture, followed by incubation for 30 min at room temperature. The OD of the reaction solution was taken at 530 nm.

2.8 Electrolyte leakage (EL)

Fresh leaf tissue (0.5 g) was chopped in uniformed discs and submerged in 10 mL deionized water in test tubes. The samples were kept for 12 h, and then EC1 was recorded. Then samples were autoclaved for 1 h and allowed to cool down at room temperature for 20 min. Then EC2 was recorded, and EL was calculated using the following equation of Lutts et al. (1995).

$$\mathrm{EL}\ (\%) = \mathrm{EC2} - \mathrm{EC1}\ /\ \mathrm{EC1} \times 100$$

2.9 Histochemical characterization for H_2O_2 and superoxide radical ($O_2^{\bullet-}$)

Fresh leaves of sesame plants were separated from plant and immersed the leaves for 24 h in dark place. Leaves were immersed in 0.1% of 3- diaminobenzidine (DAB) for the confirmation of H_2O_2 and 0.1% nitroblue tetrazolium chloride (NBT) solution for the confirmation of $O_2^{\bullet-}$. Then leaves were dipped in 95% ethanol and boiled until the green color of the leaves was fully bleached. DAB reacted with H_2O_2 and generated brown spots, while dark blue spots were generated in leaves as NBT reacted with $O_2^{\bullet-}$. Then images were made of each leaf separately.

2.10 Methylglyoxal (MG)

Ten mL of perchloric acid (5%) was used to homogenize 0.5 g of fresh leaf tissue. The homogenate was centrifuged at 10,000 rpm for 15 min, and the supernatant was collected for further use. The supernatant was thoroughly mixed with charcoal and Na_2CO_3. Then filtrate was utilized in N-acetyl-L-cysteine-based protocol at 288 nm on a spectrophotometer (Nahar et al. 2016).

2.11 Nitric oxide (NO)

Estimation of NO was carried out using protocol of Zhou et al. (2005). 0.5 g leaf tissue was homogenized in 10 mL chilled acetate buffer (50 mM), and the supernatant was collected after centrifugation. Then the supernatant was thoroughly mixed with 100 mg charcoal, and filtrate was collected after filtration. Filtrate (1 mL) was then mixed with Griess reagent (1 mL) in a test tube. The samples were allowed to incubate for 20 min at room temperature, and OD was recorded at 540 nm.

2.12 Hydrogen sulphide (H_2S)

H_2S determination was carried out by the protocol of Nashef et al. (1977). Leaf tissue (0.5 g) was finely ground in 10 mL of potassium phosphate buffer (50 mM), and the supernatant was collected after centrifugation. The supernatant (0.1 mL) was mixed with 20 mM 5,5-dithiobis-2-nitrobenzoic acid (20 µL), 50 mM of potassium phosphate buffer having pH 7.5 (0.188 mL) and deionized water 1.7 mL in test tubes. Then OD was recorded at 412 nm.

2.13 Anthocyanin

Anthocyanin was determined using the protocol of Mita et al. (1997). Leaf tissue (0.5 g) was homogenized in 10 mL of 1% acidic (HCl) methanol solution, and the supernatant was collected after centrifugation. The OD of the supernatant was recorded at 530 and 657 nm.

2.14 Flavonoids

Fresh leaf (0.5 g) was homogenized in 10 mL of 80% methanol solution, and the supernatant was collected. The reaction solution contained 4 mL deionized water and 1 mL extract, 0.3 mL of 5% $NaNO_2$, and was given incubation at 25 ºC for 5 min. Further, 0.3 mL $AlCl_3$ and 2 mL NaOH (1 M) were added. The OD was noted at 510 nm using a spectrophotometer (Zhishen et al. 1999).

2.15 Phenolics

Fresh leaf (0.5 g) was homogenized in 10 mL of 80% methanol, and the supernatant was collected after centrifugation. The reaction mixture contained 0.9 mL deionized water, 0.1 mL supernatant, 0.1 mL of Folin–Ciocalteu reagent (2 N) and was given incubation at 25 ºC for 5 min. Then 1 mL of Na_2CO_3 (7%) was added. The OD was noted at 750 nm using a spectrophotometer (Wolfe et al. 2003).

2.16 Ascorbate (ASA)

Fresh leaf tissue (0.5 g) was homogenized in 3 mL of 5% metaphosphoric acid having 1 mM EDTA. The supernatant was collected after centrifugation and used for ascorbate analysis. For total ASA determination, dithiothreitol (0.1 M)

was mixed with the reaction solution to reduce the oxidized part of ASA. The total and reduced ascorbate absorption was read at 265 nm on a spectrophotometer. Dehydroascorbate (DHA), the oxidized part of ASA, was calculated by subtracting the reduced ASA from total ASA (Hasanuzzaman et al. 2018a).

2.17 Glutathione contents

Reduced glutathione (GSH) and oxidized glutathione (GSSG) were estimated following the technique of Hasanuzzaman et al. (2011). Fresh leaf tissue was finely ground in 10 mL of metaphosphoric acid (5%) and 1 mM EDTA. After centrifugation, the supernatant was collected and mixed with potassium phosphate buffer (50 mM; pH 7.5) and 5,5-dithiobis(2-nitrobenzoic acid). Reaction mixture was used to take OD at 412 nm. For GSSG estimation, 2-vinylpyridine was added which removed GSH and OD was noted at 412 nm.

2.18 DPPH· radical activity

Fresh leaf tissue (0.5 g) was homogenized in 10 mL of 80% acetone solution to collect the supernatant. Reaction mixture contained 100 µL supernatant, 1 mL 250 mM DPPH solution and 1 mL ethanol in test tubes. The samples were incubated in dark for 30 min. The OD was recorded at 517 nm (Sarker and Oba 2018).

2.19 Total free amino acids (TFAA)

Leaf tissue (0.5 g) was finely ground in 10 mL K-P- buffer with pH 7.8. Then the homogenate was centrifuged and supernatant was obtained. Supernatant (1 mL) was reacted with 1 mL of pyridine (10%) and acid ninhydrin (1 mL) followed by incubation at 95° C for 30 min. Then, 7 mL of deionized water was added and OD was measured at 570 nm (Hamilton et al. 1943).

2.20 Total soluble sugars (TSS)

Total soluble sugars were quantified from fresh leaf material homogenized in aqueous (80%) ethanol. 100 µL of ethanolic extract was reacted with anthrone reagent (3 mL). The anthrone reagent was prepared in 72% sulfuric acid. The reaction solution was heated in a water bath at 95 °C for 10 min. The absorbance of the solution was read at 625 nm using a spectrophotometer (Yemm and Willis 1954).

2.21 Reducing sugars

The ethanolic extract (the same used for total soluble sugars) measuring 100 µL was mixed with 6% *O*-toluidine, and the resultant mixture was then heated at 95 °C for 30 min. Afterward, the reaction solution was allowed to acquire room temperature before taking OD (optical density) at 630 nm using a spectrophotometer (Nelson 1944).

2.22 Non-reducing sugars

Non-reducing sugars were quantified following formula given by Loomis and Shull (1937).

Non-reducing sugars = Total soluble sugars – reducing sugars × 0.95.

2.23 Enzyme assays

For the estimation of total soluble proteins (TSP) and enzymes activity, fresh plant tissue (0.5 g) was homogenized in 10 mL of potassium buffer (50 mM; pH 7.5). The supernatant was collected after centrifugation at 12,000 rpm for 10 min at 4° C and used in TSP and enzyme assay. Total soluble protein was determined using protocol of Bradford (1976).

SOD activity in reaction mixture was calculated by monitoring the photochemical inhibition of nitroblue tetrazolium chloride by recording OD at 560 nm (Giannopolitis and Ries 1977).

POD activity was noted by preparing total 3 mL reaction mixture, reacting 0.1 mL enzyme extract with H_2O_2 (10 mM) and guaiacol (20 mM). The increment in absorption was recorded at 470 nm (Polle et al. 1994).

CAT activity was determined using technique of Chance and Maehly (1955). Reaction mixture consisted of 0.5 M potassium phosphate buffer (7.0 pH), enzyme extract 100 µL and H_2O_2 (20 mM). Then decrease in absorbance was observed at 240 nm.

APX activity was recorded according to protocol of Nakano and Asada (1981). Reaction mixture consisted of 50 mM potassium phosphate buffer (2400 µL), 300 µL ascorbic acid (0.5 mM), 0.1 mL Na-EDTA (0.1 mM), and H_2O_2 (0.1 mM). A decrease in absorbance was observed at 290 nm.

Glutathione *S*-transferase (GST) activity was measured following the protocol of Hasanuzzaman et al. (2011). Reaction mixture contained extraction buffer (50 mM), 1.5 mM GSH (0.5 mL), (400 µL) 1-chloro-2,4-dinitrobenzene (1 mM) and 0.1 mL enzyme extract. An increase in absorbance was noted at 340 nm.

Nitrate reductase was measured by method of Joyia et al. (2021). 1 mL enzyme extract was reacted with 1% sulphanilamide solution (0.5 mL) and 0.5 mL 1-nephthyl-ethylenediamine dihydrochloride solution (0.02%). Then reaction mixture was incubated at 32° C for 30 min and OD was recorded at 542 nm.

Lipoxygenase (LOX) activity was monitored using method of Doderer et al. (1992). Enzyme extract (0.1 mL) was reacted with 0.5 mL substrate solution (linoleic acid) and distilled water 2.4 mL. The absorbance was measured at 234 nm.

Monodehydroascorbate reductase (MDHAR) activity was estimated using method of Hossain et al. (1984). The enzyme extract (0.7 mL) was reacted with Tris–HCl buffer (50 mM), NADPH (0.2 mM), 2.5 mM ASA and 0.5 unit of AO (ascorbate oxidase). By the addition of AO, reaction was initiated, and OD was noted at 340 nm.

Dehydroascorbate reductase (DHAR) activity was recorded following the technique of Nakano and Asada (1981). Reaction mixture was assayed by adding 50 mM potassium phosphate buffer, 0.1 mM dehydroascorbate (DHA) and GSH (2.5 mM). Change in absorbance was recorded at 265 nm for 2 min and activity was calculated using extinction coefficient 14 mM^{-1} cm^{-1}.

Glyoxalase I (Gly I) activity was assessed using method of Hasanuzzaman et al. (2011). Reaction mixture was prepared by adding phosphate buffer (50 mM), magnesium sulfate (15 mM), MG (3.5 mM) and GSH (1.7 mM). The reaction began when MG was added to the reaction solution and increase in absorbance was monitored at 240 nm for 60 s.

Glyoxalase II (Gly II) activity was assessed following the protocol of Principato et al. (1987). Tris–HCl buffer (100 mM) was mixed with 0.2 mM DTNB followed by 1 mM addition of *S*-D-lactoylglutathion (SLG). At 412 nm, OD was noted. With extinction coefficient 13.6 mM^{-1} cm^{-1}, Gly II activity was computed.

2.24 Ions analysis

Dry plant tissue 0.1 g (leaf and root) was digested using H_2SO_4 (2 mL) in digestion flasks. The samples were incubated for 24 h and then heated on hotplate followed by the addition of H_2O_2 (35%). The process was repeated until the digestion mixture became transparent. Then digestion solution was diluted by increasing volume up to 50 mL followed by filtration (Allen et al. 1986). Furthermore, the filtrate was used to estimate phosphorus content according to the method of Jackson (1969). Potassium (K) and calcium (Ca) ions were determined using flame photometer (Sherwood, model 410, UK). Further, Zn, Fe, Mg and Mn were determined using inductively coupled plasma spectroscopy (Teledyne Leeman Labs, Prodigy7 ICP-OES).

Nitrogen content of dry leaf tissue was estimated using protocol of Hafez and Mikkelsen (1981). Briefly, dry leaf material (0.1 g) was homogenized in 5 mL of orange dye reagent. The homogenate was filtered using Whatman no.1 filter paper and filtrate was diluted 100 times. Reaction mixture contained 2.9 mL deionized water and filtrate (30 µL). The OD was recorded at 482 nm.

2.25 Statistical analysis

Experiment was conducted in a completely randomized design with four replicates of each treatment. ANOVA of data was computed using XLSTAT software v.2017.3 (Paris, France). The differences in means were separated using least significant difference test at 95% confidence level. Correlations and principal component analysis were performed using Rstudio.

3 Results

3.1 Growth characteristics

Our results manifested a decline in shoot fresh (28.83, and 53.59%) and dry biomass (23.78 and 53.01%) relative to control in plants treated with 450 and 750 mg kg^{-1} Mn toxicity, respectively. Coumarin (50 and 100 mg L^{-1}) considerably promoted shoot fresh weight (20.19 and 34.37% under 450 mg kg^{-1} Mn; 52.01 and 87.36% under 750 mg kg^{-1} Mn, respectively) relative to unprimed plants. Similarly, COU 50 and 100 mg L^{-1} priming promoted shoot dry weight (23.84 and 19.34% under 450 mg kg^{-1} Mn; 42.06 and 29.41% under 750 mg kg^{-1} Mn, respectively) compared with control plants. Likewise, root fresh (41.88 and 52.92%) and dry weight (24.32 and 51.35%) decreased relative to control under 450 and 750 mg kg^{-1} Mn levels, respectively. COU 50 and 100 mg L^{-1} seed priming enhanced root fresh (230 and 184.15% under 450 mg kg^{-1} Mn; 130.27 and 112.38% under 750 mg kg^{-1} Mn, respectively) and dry weight (45.40 and 27.04% under 450 mg kg^{-1} Mn; 57.14 and 34.92% under 750 mg kg^{-1} Mn, respectively) compared with control plants (Table 1). Likewise, our results highlighted a conspicuous abridge ($P \leq 0.001$) in shoot (17.40 and 29.38%) and root lengths (4.27 and 24.85%) and leaf area (28.51 and 42.27%) of sesame plants under 450 and 750 mg kg^{-1} Mn toxicity, respectively. Coumarin (50 and 100 mg L^{-1}) as pre-sowing seed treatment substantially increased leaf area (35.68 and 28.72% under 450 mg kg^{-1} Mn; 34.84 and 26.34% under 750 mg kg^{-1} Mn, respectively) and shoot length (30.47 and 16.35% under 450 mg kg^{-1} Mn; 50.34 and 39.78% under 750 mg kg^{-1} Mn, respectively) and root length (34.88 and 19.68% under 450 mg kg^{-1} Mn; 33.33 and 41.86% under 750 mg kg^{-1} Mn, respectively) of sesame plants (Table 1).

Table 1 Effect of exogenous coumarin on shoot fresh weight (SFW), shoot dry weight (SDW), root fresh weight (RFW), root dry weight (RDW), shoot length (SL), and root length (RL) in sesame (*Sesamum indicum* L.) under Mn toxicity. Data are means ± standard error of four replicates ($n=4$). The values in each column followed by different letters are significantly different at 95% confidence level according to least significant difference (LSD) test. Where, ** reflects $P \leq 0.01$; *** reflects $P \leq 0.001$; ns reflects non-significant

Source of variations		SFW (g)	SDW (g)	RFW (g)	RDW (g)	SL (cm)	RL (cm)	Leaf area (cm^2)
Mn 0 mg kg^{-1} soil	Unprimed	30.79 ± 2.55^{BC}	2.98 ± 0.33^{D}	2.28 ± 0.21^{DE}	0.65 ± 0.06^{BCD}	46.28 ± 2.63^{BC}	12.88 ± 1.32^{BCDE}	31.16 ± 1.88^{BCD}
	Hydro-primed	32.80 ± 3.46^{AB}	3.03 ± 0.39^{CD}	2.32 ± 0.09^{DE}	0.64 ± 0.05^{BCDE}	51.25 ± 2.64^{ABC}	12.55 ± 1.49^{BCDE}	33.74 ± 2.16^{ABCD}
	COU 50 mg L^{-1}	40.92 ± 5.47^{A}	4.58 ± 0.20^{A}	6.26 ± 0.72^{A}	0.93 ± 0.12^{A}	54.68 ± 3.28^{A}	16.55 ± 1.78^{A}	39.86 ± 2.39^{A}
	COU 100 mg L^{-1}	40.56 ± 10.09^{A}	4.12 ± 0.21^{AB}	4.29 ± 0.43^{B}	0.77 ± 0.07^{B}	52.60 ± 1.95^{AB}	15.50 ± 1.53^{AB}	35.11 ± 3.66^{ABC}
	COU 150 mg L^{-1}	34.04 ± 1.47^{AB}	3.64 ± 0.41^{BC}	3.38 ± 0.29^{C}	0.61 ± 0.08^{CDEF}	44.58 ± 1.73^{CDE}	14.38 ± 1.64^{ABC}	36.86 ± 2.26^{AB}
Mn 450 mg kg^{-1} soil	Unprimed	21.91 ± 1.66^{CDE}	2.28 ± 0.08^{EF}	1.33 ± 0.23^{F}	0.49 ± 0.05^{DEFG}	38.23 ± 1.27^{EF}	12.33 ± 0.88^{BCDE}	22.28 ± 2.79^{FGH}
	Hydro-primed	21.70 ± 2.39^{DE}	2.29 ± 0.28^{EF}	1.59 ± 0.16^{EF}	0.48 ± 0.05^{FG}	38.92 ± 4.02^{DEF}	12.68 ± 2.09^{BCDE}	20.92 ± 0.93^{GH}
	COU 50 mg L^{-1}	26.34 ± 1.80^{BCD}	2.82 ± 0.28^{DE}	4.37 ± 0.36^{B}	0.71 ± 0.06^{BC}	49.88 ± 2.77^{ABC}	16.63 ± 1.03^{A}	30.23 ± 2.36^{CDE}
	COU 100 mg L^{-1}	29.44 ± 2.0^{BCD}	2.72 ± 0.21^{DE}	3.77 ± 0.09^{BC}	0.62 ± 0.05^{BCDEF}	44.48 ± 3.41^{CDE}	14.75 ± 1.59^{ABC}	28.68 ± 1.98^{DEF}
	COU 150 mg L^{-1}	16.52 ± 2.71^{E}	1.98 ± 0.18^{FG}	2.33 ± 0.27^{DE}	0.37 ± 0.07^{GH}	32.50 ± 3.18^{F}	9.70 ± 0.87^{E}	20.08 ± 2.50^{GH}
Mn 750 mg kg^{-1} soil	Unprimed	14.29 ± 1.69^{E}	1.40 ± 0.13^{GH}	1.09 ± 0.24^{F}	0.32 ± 0.04^{H}	32.68 ± 2.77^{F}	9.68 ± 1.62^{E}	17.99 ± 1.94^{GH}
	Hydro-primed	15.7 ± 3.52^{E}	1.53 ± 0.10^{GH}	1.31 ± 0.16^{F}	0.29 ± 0.03^{H}	35.83 ± 2.35^{F}	10.80 ± 0.89^{DE}	17.02 ± 3.38^{H}
	COU 50 mg L^{-1}	21.72 ± 1.90^{DE}	1.99 ± 0.33^{FG}	2.51 ± 0.46^{D}	0.49 ± 0.04^{DEFG}	49.13 ± 2.48^{ABC}	12.90 ± 1.03^{BCDE}	24.25 ± 2.84^{EFG}
	COU 100 mg L^{-1}	26.78 ± 1.02^{BCD}	1.82 ± 0.16^{FG}	2.32 ± 0.11^{DE}	0.43 ± 0.04^{GH}	45.68 ± 4.15^{BCD}	13.73 ± 1.14^{ABCD}	22.73 ± 3.57^{FGH}
	COU 150 mg L^{-1}	14.97 ± 2.32^{E}	1.18 ± 0.06^{H}	1.23 ± 0.19^{F}	0.29 ± 0.04^{H}	31.83 ± 4.19^{F}	11.40 ± 0.91^{CDE}	19.63 ± 2.90^{GH}
ANOVA	Priming treatments (PT)	***	***	***	***	***	***	***
	Manganese toxicity (Mn)	***	***	***	***	***	**	***
	PT × Mn	ns	ns	***	ns	ns	ns	ns

3.2 SPAD values and photosynthetic pigments

A remarkable decline in SPAD values (24 and 54.81%) compared with control was observed in plants subjected to 450 and 750 mg kg^{-1} Mn, respectively. Coumarin (50 and 100 mg L^{-1}) treated plants showed greater SPAD values (40.44 and 31.96% under 450 mg kg^{-1} Mn; 92.97 and 65.33% under mg kg^{-1} Mn, respectively) (Table 2).

A significant fall in chlorophyll *a* (11.75 and 35.31%) *b* (17.64 and 29.64%) and total chlorophyll (13.54 and 33.58%) values was evident in plants exposed to 450 and 750 mg kg^{-1} Mn toxicity, respectively. Coumarin (50, 100, and 150 mg L^{-1}) remarkably improved chlorophyll *a* (26.21, 24.76 and 8.35% under 450 mg kg^{-1} Mn; 57.90, 40.37 and 11.86% mg kg^{-1} Mn, respectively), *b* (37.27, 25.79 and 15.93% under 450 Mn; 35.77, 17.15 and 0.272% under 750 mg kg^{-1} Mn levels, respectively) and total chlorophyll (29.42, 25.06 and 10.54% under 450 mg kg^{-1} Mn; 50.77, 32.89 and 8.12% under 750 mg kg^{-1} Mn, respectively) in sesame. Besides, Chl. ab^{-1} did not show any effect of either Mn toxicity or COU (Table 1). Additionally, carotenoid contents increased (10.38 and 45.33%) in sesame plants under 450 and 750 mg kg^{-1} Mn levels, respectively. Coumarin (50, 100, and 150 mg L^{-1}) produced several folds rise (76.17, 40.49 and 16.02% under 450 mg kg^{-1} Mn; 24.43, 26.45 and 5.09% under 750 mg kg^{-1} Mn levels, respectively) in the carotenoid values as compared to unprimed plants (Table 2).

3.3 Gas exchange characteristics

Photosynthesis decreased drastically (41.55 and 64.65%) in sesame plants on exposure to 450 and 750 mg kg^{-1} Mn stress, respectively. Further, COU (50, 100 and 150 mg L^{-1}) persuaded a several folds upsurge (31.31, 28.07 and 21.84%

Table 2 Effect of exogenous coumarin on photosynthetic pigments in sesame (*Sesamum indicum* L.) under Mn toxicity. Data are means ± standard error of four replicates ($n=4$). The values in each column followed by different letters are significantly different at 95% confidence level according to least significant difference (LSD) test. Where, ** reflects $P \leq 0.01$; *** reflects $P \leq 0.001$; ns reflects non-significant

Source of variations		SPAD value	Chl. *a* (mg g^{-1} FW)	Chl. *b* (mg g^{-1} FW)	T. Chl. (mg g^{-1} FW)	Chl. ab^{-1}	Carotenoid (mg g^{-1} FW)
Mn 0 mg kg^{-1} soil	Unprimed	17.33 ± 0.93^{BCD}	1.11 ± 0.05^{BCD}	0.48 ± 0.024^{ABCD}	1.59 ± 0.08^{BCD}	2.29 ± 0.03^{A}	0.003 ± 0.0006^{EF}
	Hydro-primed	17.37 ± 2.31^{BC}	0.99 ± 0.08^{DE}	0.44 ± 0.05^{CD}	1.42 ± 0.13^{D}	2.28 ± 0.08^{A}	0.003 ± 0.0005^{DEF}
	COU 50 mg L^{-1}	25.04 ± 2.20^{A}	1.25 ± 0.08^{AB}	0.53 ± 0.01^{AB}	1.78 ± 0.07^{AB}	2.37 ± 0.20^{A}	0.004 ± 0.0006^{CDEF}
	COU 100 mg L^{-1}	26.37 ± 2.45^{A}	1.35 ± 0.18^{A}	0.53 ± 0.04^{AB}	1.88 ± 0.16^{A}	2.61 ± 0.53^{A}	0.004 ± 0.0008^{BCDE}
	COU 150 mg L^{-1}	20.83 ± 0.73^{B}	1.03 ± 0.02^{CD}	0.46 ± 0.01^{BCD}	1.49 ± 0.04^{CD}	2.25 ± 0.01^{A}	$0.003 \pm 0.0005F$
Mn 450 mg kg^{-1} soil	Unprimed	13.17 ± 2.45^{EF}	0.98 ± 0.05^{DE}	0.39 ± 0.02^{DE}	1.37 ± 0.06^{DE}	2.48 ± 0.24^{A}	0.004 ± 0.0006^{CDEF}
	Hydro-primed	12.40 ± 2.25^{EFG}	0.99 ± 0.11^{DE}	0.41 ± 0.05^{DE}	1.41 ± 0.15^{D}	2.42 ± 0.20^{A}	0.004 ± 0.0005^{CDEF}
	COU 50 mg L^{-1}	18.50 ± 1.63^{BC}	1.23 ± 0.10^{ABC}	0.54 ± 0.05^{A}	1.77 ± 0.06^{AB}	2.34 ± 0.42^{A}	0.006 ± 0.0006^{A}
	COU 100 mg L^{-1}	17.38 ± 1.73^{BC}	1.22 ± 0.09^{ABC}	0.50 ± 0.03^{ABC}	1.71 ± 0.09^{ABC}	2.46 ± 0.29^{A}	0.005 ± 0.0007^{ABC}
	COU 150 mg L^{-1}	13.26 ± 0.91^{DEF}	1.06 ± 0.05^{BCD}	0.46 ± 0.02^{ABCD}	1.51 ± 0.07^{CD}	2.29 ± 0.04^{A}	0.004 ± 0.0007^{CDEF}
Mn 750 mg kg^{-1} soil	Unprimed	7.83 ± 1.34^{H}	0.72 ± 0.05^{F}	0.34 ± 0.02^{E}	1.06 ± 0.04^{F}	2.14 ± 0.26^{A}	0.005 ± 0.0002^{BCDE}
	Hydro-primed	8.98 ± 0.85^{GH}	0.81 ± 0.07^{EF}	0.33 ± 0.05^{E}	1.15 ± 0.07^{EF}	2.60 ± 0.50^{A}	0.005 ± 0.0007^{BCD}
	COU 50 mg L^{-1}	15.12 ± 1.55^{CDE}	1.13 ± 0.06^{BCD}	0.46 ± 0.05^{ABCD}	1.59 ± 0.11^{BCD}	2.50 ± 0.22^{A}	0.005 ± 0.0005^{AB}
	COU 100 mg L^{-1}	12.95 ± 0.81^{EFG}	1.00 ± 0.05^{DE}	0.39 ± 0.01^{DE}	1.40 ± 0.04^{D}	2.54 ± 0.20^{A}	0.006 ± 0.0006^{AB}
	COU 150 mg L^{-1}	9.57 ± 0.62^{FGH}	0.80 ± 0.08^{EF}	0.34 ± 0.02^{E}	1.14 ± 0.07^{F}	2.36 ± 0.29^{A}	0.005 ± 0.0002^{ABCD}
ANOVA	Priming treatments (PT)	***	***	***	***	ns	**
	Manganese toxicity (Mn)	***	***	***	***	ns	***
	PT × Mn	ns	ns	ns	ns	ns	ns

under 450 mg kg^{-1} Mn; 72.87, 68.74 and 46.33% under 750 mg kg^{-1} Mn, respectively) in photosynthesis of sesame plants relative to control (Fig. 1).

A significant drop in transpiration rate (13.63 and 51.36%) was present in sesame plants under 450 and 750 mg kg^{-1} Mn toxicity, respectively. Besides, plants administered with COU 50, 100 and 150 mg L^{-1} manifested a decline (23.68, 23.68 and 18.42% under 450 mg kg^{-1} Mn; 27.57, 34.11 and 38.16% under 750 mg kg^{-1} Mn, respectively) in this attribute under Mn stress (Fig. 1).

Our results revealed a notable drop in stomatal conductance (22.32 and 29.55%) in sesame plants under 450 and 750 mg kg^{-1} Mn, respectively. Further, COU (50 and 100 mg L^{-1}) persuaded a marked improvement (51.02 and 24.01% under 450 mg kg^{-1} Mn; 42.87 and 36.41% under 750 mg kg^{-1} Mn, respectively) in stomatal conductance compared with unprimed plants (Fig. 1).

Water use efficiency (WUE) of sesame plants dropped conspicuously (30.45 and 27.75%) under 450 and 750 mg kg^{-1} Mn stress, respectively. Besides, COU (50, 100 and 150 mg L^{-1}) significantly improved WUE (66.63, 64.29 and 49.07% under 450 mg kg^{-1} Mn; 139.39, 161.56 and 135.85% under 750 mg kg^{-1} Mn, respectively) compared with control plants (Fig. 1).

3.4 Antioxidant pigments

Manganese toxicity significantly decreased (19.75 and 32.60%) β-carotene in sesame plants under 450 and 750 mg kg^{-1} Mn, respectively. Coumarin (50 and 100 mg L^{-1}) showed maximal increment (66.51 and 53.57% under 450 mg kg^{-1} Mn; 44.85 and 30.19% under 750 mg kg^{-1} Mn, respectively) relative to unprimed plants. Besides, β-cyanin (35.19 and 66.27%) and β-xanthin (31.35 and 63.27%) increased in sesame plants under 450 and 750 mg kg^{-1} Mn, respectively. Coumarin (50, 100,

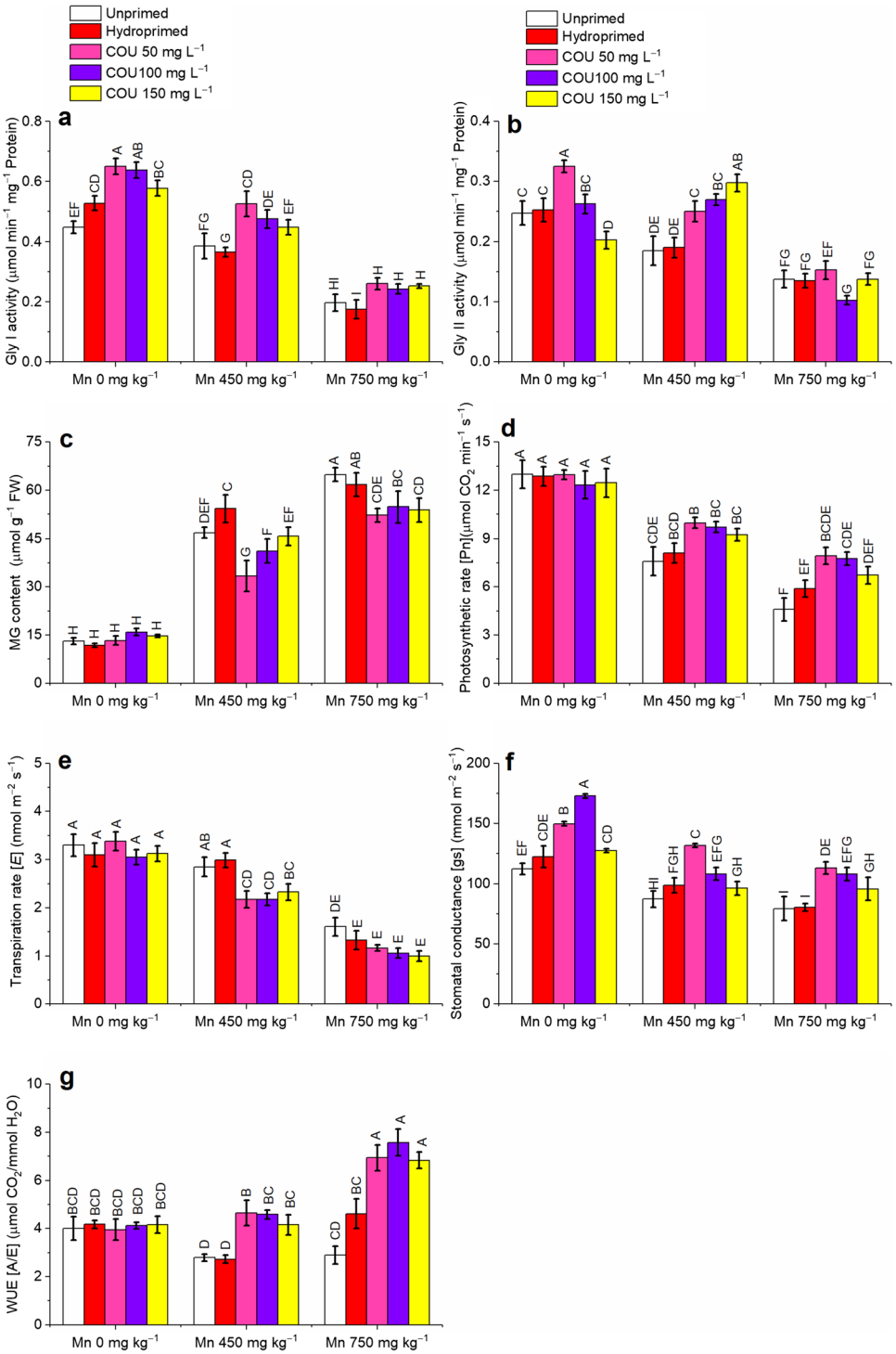

Fig. 1 Coumarin-mediated modifications in gas exchange attributes and glyoxal system in sesame (*Sesamum indicum* L.) under Mn toxicity. Uppercase letters represent significance at 95% confidence level

and 150 mg L^{-1}) produced a several folds increase in β-cyanin (46.2, 32.53 and 23.21% under 450 mg kg^{-1} Mn; 35.27, 29.27 and 24.51% under 750 mg kg^{-1} Mn, respectively) and β-xanthin values (44.3, 35.05 and 25.59% under 450 mg kg^{-1} Mn; 33.91, 27.88 and 23.18% under 750 mg kg^{-1} Mn) relative to unprimed sesame plants (Table 3).

3.5 Soluble sugars

Plants accumulated a significant amount of total soluble sugars (15.60 and 38.47%) in response to 450 and 750 mg kg^{-1} Mn toxicity levels, respectively. Coumarin (50 and 100 mg L^{-1}) markedly increased soluble sugars (56.47

Table 3 Effect of exogenous coumarin on antioxidant pigments, total soluble sugars (TSS), reducing sugars (RS), non-reducing sugars (NRS) in sesame (*Sesamum indicum* L.) under Mn toxicity. Data are means ± standard error of four replicates ($n = 4$). The values in each column followed by different letters are significantly different at 95% confidence level according to least significant difference (LSD) test. * means $P \leq 0.05$; ** reflects $P \leq 0.01$; *** reflects $P \leq 0.001$; ns reflects non-significant

Source of variations		β-carotene (μg g^{-1} FW)	β-cyanine (ng g^{-1} FW)	β-xanthin (ng g^{-1} FW)	TSS (mg g^{-1} FW)	RS (mg g^{-1} FW)	NRS (mg g^{-1} FW)
Mn 0 mg kg^{-1} soil	Unprimed	0.07 ± 0.002^{BC}	13.75 ± 2.57^{G}	18.44 ± 3.27^{F}	15.91 ± 1.59^{G}	0.58 ± 0.05^{G}	15.33 ± 1.60^{F}
	Hydro-primed	0.06 ± 0.008^{CD}	18.02 ± 1.85^{FG}	23.59 ± 2.24^{EF}	19.15 ± 2.15^{FG}	0.61 ± 0.02^{FG}	18.54 ± 2.13^{EF}
	COU 50 mg L^{-1}	0.06 ± 0.005^{CD}	17.66 ± 0.99^{FG}	22.08 ± 1.14^{EF}	22.82 ± 1.20^{CDEF}	0.69 ± 0.10^{EFG}	22.13 ± 1.24^{BCDE}
	COU 100 mg L^{-1}	0.05 ± 0.006^{CDE}	18.47 ± 0.84^{F}	23.28 ± 1.20^{EF}	22.79 ± 1.22^{CDEF}	0.64 ± 0.01^{FG}	22.14 ± 1.24^{BCDE}
	COU 150 mg L^{-1}	0.04 ± 0.007^{DE}	18.95 ± 0.95^{EF}	23.70 ± 1.34^{EF}	18.87 ± 1.12^{FG}	0.66 ± 0.03^{FG}	18.21 ± 1.13^{EF}
Mn 450 mg kg^{-1} soil	Unprimed	0.05 ± 0.006^{CDE}	18.58 ± 0.89^{EF}	24.21 ± 1.37^{E}	18.39 ± 1.72^{FG}	0.73 ± 0.05^{DEFG}	17.66 ± 1.75^{EF}
	Hydro-primed	0.05 ± 0.003^{CDE}	19.44 ± 0.80^{DEF}	25.15 ± 0.95^{DE}	20.92 ± 1.24^{EF}	0.75 ± 0.02^{CDEF}	20.16 ± 1.23^{DE}
	COU 50 mg L^{-1}	0.09 ± 0.012^{A}	27.18 ± 2.42^{ABC}	34.95 ± 3.24^{ABC}	28.78 ± 0.76^{AB}	1.13 ± 0.09^{B}	27.64 ± 0.68^{A}
	COU 100 mg L^{-1}	0.09 ± 0.013^{AB}	24.64 ± 2.99^{BC}	32.70 ± 3.62^{BC}	27.08 ± 1.71^{ABC}	0.86 ± 0.06^{CD}	26.21 ± 1.74^{AB}
	COU 150 mg L^{-1}	0.04 ± 0.006^{E}	22.90 ± 0.86^{CDE}	30.41 ± 0.64^{CD}	22.22 ± 2.86^{DEF}	0.66 ± 0.01^{FG}	21.56 ± 2.85^{BCDE}
Mn 750 mg kg^{-1} soil	Unprimed	0.05 ± 0.007^{DE}	22.86 ± 3.00^{CDE}	30.10 ± 3.66^{CD}	22.03 ± 1.53^{DEF}	0.89 ± 0.03^{C}	21.13 ± 1.52^{CDE}
	Hydro-primed	0.04 ± 0.010^{DE}	23.43 ± 2.38^{CD}	32.19 ± 2.90^{BC}	24.28 ± 1.98^{BCDE}	0.85 ± 0.06^{CDE}	23.43 ± 1.98^{ABCD}
	COU 50 mg L^{-1}	0.06 ± 0.009^{BC}	30.93 ± 0.54^{A}	40.31 ± 0.66^{A}	29.30 ± 2.16^{A}	1.36 ± 0.13^{A}	27.94 ± 2.13^{A}
	COU 100 mg L^{-1}	0.06 ± 0.008^{CD}	29.55 ± 0.33^{A}	38.50 ± 0.94^{A}	28.05 ± 3.31^{AB}	1.17 ± 0.03^{B}	26.88 ± 3.28^{A}
	COU150 mg L^{-1}	0.04 ± 0.004^{E}	28.47 ± 1.49^{AB}	37.08 ± 2.99^{AB}	26.34 ± 2.33^{ABCD}	0.89 ± 0.11^{C}	25.44 ± 2.35^{ABC}
ANOVA	Priming treatments (PT)	***	***	***	***	***	***
	Manganese toxicity (Mn)	**	***	***	***	***	***
	PT × Mn	**0.013	ns	ns	ns	**	ns

and 47.23% under 450 mg kg^{-1} Mn; 32.98 and 27.31% under 750 mg kg^{-1} Mn, respectively) relative to control. Similarly, our results revealed a conspicuous rise in reducing (25.83 and 54.72%) and non-reducing (15.22 and 37.86%) sugars in sesame plants under 450 and 750 mg kg^{-1} Mn levels, respectively. Coumarin (50 and 100 mg L^{-1}) priming showed higher values (55.79 and 19.14% under 450 mg kg^{-1} Mn; 51.41 and 30.03% under 750 mg kg^{-1} Mn, respectively) for reducing and non-reducing sugars (56.5 and 48.39% under 450 mg kg^{-1} Mn; 32.2 and 27.19% under750 mg kg^{-1} Mn, respectively) compared with unprimed plants (Table 3).

3.6 Total free amino acids (TFAA)

Manganese toxicity significantly increased TFAA (37.51 and 101.45%) in sesame plants grown under 450 and 750 mg kg^{-1} Mn levels, respectively. Coumarin (50, 100, and 150 mg L^{-1}) considerably improved (138.47, 70.98 and 40.16% under 450 mg kg^{-1} Mn; 42.83, 37.24 and 21.67% under 750 mg kg^{-1} Mn, respectively) TFAA levels compared with unprimed plants under Mn toxicity (Table 4).

3.7 Total soluble proteins (TSP)

Our results revealed a conspicuous drop (25.04%) in total soluble proteins (TSP) in sesame plants under 450 mg kg^{-1} Mn. However, a substantial upsurge (17.55%) in TSP values was evident in plants exposed to higher Mn level 750 mg kg^{-1}. Coumarin (50, 100, and 150 mg L^{-1}) significantly increased TSP (35.78, 23.72 and 14.35%, respectively) under lower Mn level (450 mg kg^{-1} Mn), whereas a fall in TSP (7.69, 7.94 and 16.8%, respectively) was observed under 750 mg kg^{-1} Mn as compared with control (Table 4).

3.8 DPPH· radical scavenging activity

Manganese toxicity diminished the total antioxidant activity of sesame plants reflected as fall in DPPH· free

Table 4 Effect of exogenous coumarin on phenolics, flavonoids, DPPH radical scavenging activity, anthocyanin, total free amino acids (TFAA), and total soluble proteins (TSP) in sesame (*Sesamum indicum* L.) under Mn toxicity. Data are means ± standard error of four replicates ($n=4$). The values in each column followed by different letters are significantly different at 95% confidence level according to least significant difference (LSD) test. Where, ** reflects $P \leq 0.01$; *** reflects $P \leq 0.001$; ns reflects non-significant

Source of variations		Phenolics (mg g^{-1} FW)	Flavonoids (µg g^{-1} FW)	DPPH (%)	Anthocyanin (Units g^{-1} FW)	TFAA (mg g^{-1} FW)	TSP (mg g^{-1} FW)
Mn 0 mg kg^{-1} soil	Unprimed	26.32 ± 2.62^{H}	0.00046 ± 6.74^{GH}	34.23 ± 1.29^{CDE}	0.96 ± 0.15^{G}	0.43 ± 0.10^{G}	3.62 ± 0.26^{BCD}
	Hydro-primed	26.53 ± 0.73^{H}	0.00049 ± 4.64^{FGH}	34.15 ± 0.64^{CDE}	1.47 ± 0.07^{EFG}	0.60 ± 0.03^{EFG}	3.49 ± 0.21^{BCD}
	COU 50 mg L^{-1}	30.85 ± 2.04^{FGH}	0.00056 ± 9.53^{DEFG}	34.15 ± 0.85^{CDE}	1.15 ± 0.22^{FG}	0.54 ± 0.03^{FG}	3.57 ± 0.24^{BCD}
	COU 100 mg L^{-1}	36.17 ± 3.27^{CDEFG}	0.00039 ± 3.77^{H}	32.70 ± 1.58^{DE}	1.60 ± 0.10^{EF}	0.61 ± 0.03^{EFG}	3.49 ± 0.30^{BCD}
	COU 150 mg L^{-1}	28.57 ± 2.02^{GH}	0.00038 ± 5.06^{H}	34.85 ± 0.83^{BCDE}	1.06 ± 0.20^{FG}	0.57 ± 0.08^{FG}	4.01 ± 0.33^{AB}
Mn 450 mg kg^{-1} soil	Unprimed	31.63 ± 3.31^{EFGH}	0.00053 ± 4.90^{EFGH}	30.85 ± 3.54^{DE}	1.74 ± 0.32^{E}	0.59 ± 0.09^{FG}	2.71 ± 0.31^{E}
	Hydro-primed	32.59 ± 4.40^{DEFGH}	0.00056 ± 3.44^{DEFG}	33.68 ± 3.05^{DE}	1.96 ± 0.38^{DE}	0.75 ± 0.10^{DEF}	2.73 ± 0.27^{E}
	COU 50 mg L^{-1}	42.27 ± 4.28^{ABC}	0.00069 ± 0.0001^{CD}	40.50 ± 3.02^{AB}	2.57 ± 0.15^{C}	1.41 ± 0.16^{A}	3.68 ± 0.31^{ABC}
	COU 100 mg L^{-1}	38.24 ± 3.18^{BCDEF}	0.00068 ± 7.44^{CDE}	41.15 ± 2.12^{A}	2.31 ± 0.10^{CD}	1.01 ± 0.04^{BC}	3.35 ± 0.28^{CD}
	COU 150 mg L^{-1}	31.25 ± 3.04^{EFGH}	0.00050 ± 4.03^{FGH}	40.15 ± 0.34^{ABC}	2.33 ± 0.09^{CD}	0.83 ± 0.11^{CDE}	3.10 ± 0.30^{DE}
Mn 750 mg kg^{-1} soil	Unprimed	39.56 ± 3.45^{BCD}	0.00071 ± 3.60^{BCD}	25.80 ± 2.28^{F}	2.38 ± 0.28^{CD}	0.87 ± 0.13^{CD}	4.26 ± 0.05^{A}
	Hydro-primed	41.15 ± 3.48^{ABC}	0.00073 ± 3.38^{BC}	26.55 ± 2.37^{F}	2.72 ± 0.23^{C}	0.90 ± 0.12^{CD}	4.06 ± 0.06^{AB}
	COU 50 mg L^{-1}	48.74 ± 2.60^{A}	0.00107 ± 6.12^{A}	36.70 ± 3.57^{ABCD}	4.30 ± 0.21^{A}	1.23 ± 0.04^{AB}	3.93 ± 0.04^{ABC}
	COU 100 mg L^{-1}	45.69 ± 2.38^{AB}	0.00085 ± 8.96^{B}	34.35 ± 3.21^{CDE}	3.41 ± 0.12^{B}	1.19 ± 0.12^{AB}	3.91 ± 0.04^{ABC}
	COU150 mg L^{-1}	38.90 ± 3.76^{BCDE}	0.00064 ± 8.30^{CDEF}	30.53 ± 3.92^{EF}	3.28 ± 0.30^{B}	1.06 ± 0.10^{BC}	3.54 ± 0.02^{BCD}
ANOVA	Priming treatments (PT)	***	***	***	***	***	ns
	Manganese toxicity (Mn)	***	***	***	***	***	***
	PT × Mn	ns	ns	ns	***	**	**

radical scavenging activity. Plants subjected to various Mn levels (450 and 750 mg kg^{-1}) displayed a significant abridge (9.86 and 24.61%, respectively) in DPPH· free radical scavenging activity. Coumarin (50, 100, and 150 mg L^{-1}) increased total antioxidant activity by several folds (31.28, 33.38 and 30.14% under 450 mg kg^{-1} Mn; 42.24, 33.13 and 18.31 under 750 mg kg^{-1} Mn, respectively) in sesame plants relative to control (Table 4).

3.9 Non-enzymatic antioxidants

Plants subjected to Mn levels (450 and 750 mg kg^{-1} Mn) displayed a significant increase (20.13 and 50.26%, respectively) in phenolics. Coumarin (50 and 100 mg L^{-1}) increased phenolics (33.68 and 20.91% under 450 mg kg^{-1} Mn; 23.2 and 15.52% under 750 mg kg^{-1} Mn, respectively) compared with control plants (Table 4).

Our results manifested a significant increase (13.56 and 53.06%) in flavonoid contents in sesame plants on exposure to 450 and 750 mg kg^{-1} Mn, respectively. Coumarin (50 and 100 mg L^{-1}) notably improved (30.63 and 29.41% under 450 mg kg^{-1} Mn; 51.94 and 19.43% under 750 mg kg^{-1} Mn, respectively) flavonoid contents in sesame plants over unprimed (Table 4).

Anthocyanins level increased significantly (80.51 and 147.27%) in sesame plants under two Mn levels (450 and 750 mg kg^{-1}, respectively). Coumarin (50,100 and 150 mg L^{-1}) noticeably enhanced (48.07, 32.66 and 33.81% under 450 mg kg^{-1} Mn; 80.56, 43.38 and 37.81% under 750 mg kg^{-1} Mn, respectively) anthocyanin contents over unprimed plants (Table 4).

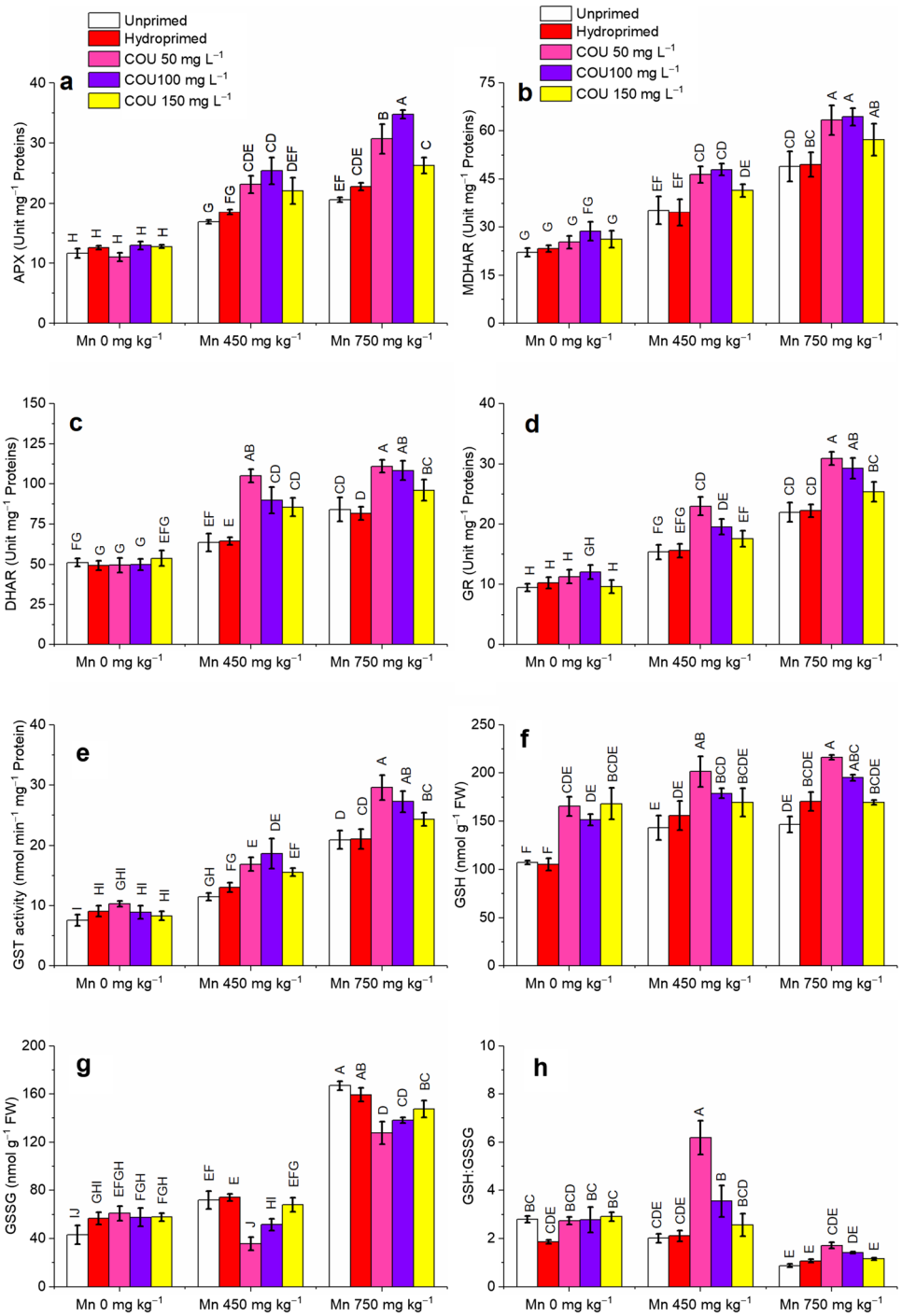

Fig. 2 Coumarin-mediated modulations in antioxidant enzyme activities and glutathione metabolism in sesame (*Sesamum indicum* L.) under Mn toxicity. Uppercase letters on standard error bars represent significance among treatments at 95% confidence level

Glutathione content increased (33.49 and 36.63%) remarkably in plants under 450 and 750 mg kg^{-1} Mn, respectively. Coumarin (50, 100, and 150 mg L^{-1}) depicted a marked increase (40.65, 24.91 and 18.22% under 450 mg kg^{-1} Mn; 47.49, 33.1 and 15.65% under 750 mg kg^{-1} Mn, respectively) in glutathione levels over control plants (Fig. 2).

Total ascorbate contents diminished noticeably (22.44 and 36.98%) in sesame plants under various Mn levels (450 and 750 mg kg^{-1} Mn, respectively). Further, COU (50 and 100 mg L^{-1}) induced a visible increase (22.54 and 26.41% under 450 mg kg^{-1} Mn; 41.82 and 33.09% under 750 mg kg^{-1} Mn, respectively) in total ascorbate contents compared with unprimed plants (Figure S5; Appendix-III).

Dehydroascorbate (DHA) exhibited a significant rise (120.88 and 167.77%) in sesame plants grown under 450 and 750 mg kg^{-1} Mn, respectively. Exogenous coumarin (50 and 100 mg L^{-1}) showed a noticeable fall (33.65 and

37.11% under 450 mg kg^{-1} Mn; 12.54 and 16.10% under 750 mg kg^{-1} Mn, respectively) in DHA content relative to control plants (Figure S5; Appendix-III).

Our results manifested a conspicuous fall (64.89 and 76.68%,) in ASA/DHA ratio in plants under 450 and 750 mg kg^{-1} Mn, respectively. Coumarin priming (50 and 100 mg L^{-1}) brought a substantial upsurge in ASA/DHA ratio (81.10 and 101.3% under 450 mg kg^{-1} Mn; 60.43 and 57.42% under 750 mg kg^{-1} Mn, respectively) relative to unprimed plants (Appendix-III).

3.10 Oxidative stress indicators

Electrolyte leakage (EL) of membranes increased significantly (157.14 and 193.88%) in sesame plants after exposure to 450 and 750 mg kg^{-1} Mn, respectively. COU (50, 100 and 150 mg L^{-1}) administration remarkably abridged membrane electrolyte leakage (33.37, 26.12 and 22.83% under 450 mg kg^{-1} Mn; 22.97, 21.94 and 15% under 750 mg kg^{-1} Mn, respectively) relative to control plants (Table 5).

The loss of membrane integrity was assessed by measuring the endogenous malondialdehyde (MDA) levels in plants under Mn toxicity. The rise in MDA values was concentration-dependent as maximal MDA values (180.06 and 318.98%) were evident in plants stressed with 450 and 750 mg kg^{-1} Mn levels, respectively. Further, COU (50 and 100 mg L^{-1}) priming resulted in a noteworthy lessening (33.33 and 38.71% under 450 mg kg^{-1} Mn; 45.09 and 31.34% under 750 mg kg^{-1} Mn, respectively) in MDA production relative to unprimed plants (Table 5).

A marked increase (25.89 and 69.6%) occurred in H_2O_2 production in sesame plants upon exposure to 450 and

Table 5 Effect of exogenous coumarin on electrolyte leakage (EL), malondialdehyde (MDA), hydrogen peroxide (H_2O_2), superoxide radical ($O_2^{\bullet-}$), lipoxygenase activity (LOX), ascorbic acid (AsA), and glycine betaine (GB) in sesame (*Sesamum indicum* L.) under Mn toxicity. Data are means ± standard error of four replicates ($n = 4$). The values in each column followed by different letters are significantly different at 95% confidence level according to least significant difference (LSD) test. ** reflects $P \leq 0.01$; *** reflects $P \leq 0.001$; ns reflects non-significant

Source of variations		EL (%)	MDA (nmol ml^{-1} g^{-1} FW)	H_2O_2 (nmol g^{-1} FW)	$O_2^{\bullet-}$ (nmol g^{-1} FW)	LOX (µmol min^{-1} mg^{-1} proteins)	RWC (%)	GB (µg g^{-1} FW)
Mn 0 mg kg^{-1} soil	Unprimed	12.73 ± 1.91^{G}	20.25 ± 2.23^{F}	157.27 ± 7.56^{C}	7.54 ± 0.38^{E}	19.28 ± 1.88^{G}	86.30 ± 3.76^{A}	30.21 ± 1.96^{E}
	Hydro-primed	11.36 ± 1.66^{G}	23.40 ± 3.66^{F}	157.27 ± 6.99^{C}	7.21 ± 0.18^{E}	18.73 ± 0.92^{G}	83.89 ± 4.13^{ABC}	30.48 ± 2.79^{E}
	COU 50 mg L^{-1}	12.42 ± 2.15^{G}	20.93 ± 1.99^{F}	145.61 ± 2.95^{C}	6.60 ± 0.15^{E}	19.59 ± 1.49^{G}	84.01 ± 2.40^{ABC}	31.32 ± 0.68^{DE}
	COU 100 mg L^{-1}	16.22 ± 2.39^{FG}	20.44 ± 3.09^{F}	151.14 ± 3.85^{C}	6.82 ± 0.16^{E}	22.49 ± 2.65^{FG}	85.83 ± 3.21^{AB}	32.42 ± 0.64^{CDE}
	COU 150 mg L^{-1}	14.57 ± 2.05^{G}	19.90 ± 1.12^{F}	169.32 ± 4.15^{C}	7.82 ± 0.36^{E}	20.79 ± 2.03^{G}	80.70 ± 4.50^{ABCD}	37.49 ± 2.39^{C}
Mn 450 mg kg^{-1} soil	Unprimed	32.76 ± 3.27^{BC}	56.73 ± 3.17^{BC}	198.01 ± 16.70^{B}	19.30 ± 1.43^{BC}	36.39 ± 1.98^{CD}	68.23 ± 2.92^{EFGH}	36.68 ± 0.90^{CD}
	Hydro-primed	33.36 ± 3.17^{BC}	43.33 ± 3.49^{DE}	205.37 ± 9.80^{B}	18.18 ± 0.83^{BC}	36.88 ± 3.95^{CD}	65.77 ± 5.54^{FGHI}	37.46 ± 1.56^{CD}
	COU 50 mg L^{-1}	21.82 ± 2.03^{EF}	37.82 ± 5.12^{DE}	169.76 ± 9.73^{C}	13.36 ± 1.77^{D}	22.73 ± 2.74^{FG}	76.93 ± 2.14^{BCDE}	47.99 ± 4.97^{B}
	COU 100 mg L^{-1}	24.20 ± 2.30^{DE}	34.77 ± 2.37^{E}	166.08 ± 9.01^{C}	12.36 ± 1.76^{D}	28.39 ± 1.69^{EF}	75.46 ± 3.60^{CDE}	47.28 ± 4.40^{B}
	COU 150 mg L^{-1}	25.27 ± 2.80^{DE}	45.38 ± 4.77^{D}	203.60 ± 2.13^{B}	16.54 ± 1.71^{CD}	31.90 ± 2.40^{DE}	65.54 ± 3.21^{FGHI}	44.63 ± 1.68^{B}
Mn 750 mg kg^{-1} soil	Unprimed	37.44 ± 2.83^{AB}	84.87 ± 4.41^{A}	266.74 ± 12.85^{A}	33.06 ± 2.28^{A}	56.70 ± 4.76^{A}	57.85 ± 4.44^{I}	47.41 ± 1.76^{B}
	Hydro-primed	39.97 ± 1.98^{A}	80.60 ± 7.60^{A}	253.74 ± 7.12^{A}	31.37 ± 2.81^{A}	55.51 ± 4.80^{A}	59.76 ± 1.60^{HI}	50.09 ± 2.08^{B}
	COU 50 mg L^{-1}	28.83 ± 2.80^{CD}	46.60 ± 2.72^{CD}	206.95 ± 17.47^{B}	21.91 ± 2.99^{B}	43.03 ± 4.49^{BC}	73.49 ± 3.31^{DEF}	56.38 ± 1.66^{A}
	COU 100 mg L^{-1}	29.22 ± 2.84^{CD}	58.27 ± 7.61^{B}	212.96 ± 20.67^{B}	20.47 ± 2.63^{BC}	41.62 ± 3.29^{BC}	70.06 ± 5.29^{EFG}	59.45 ± 3.59^{A}
	COU150 mg L^{-1}	31.78 ± 2.70^{BC}	64.97 ± 4.13^{B}	248.82 ± 4.27^{A}	30.49 ± 2.99^{A}	47.62 ± 2.28^{B}	62.22 ± 3.17^{GHI}	47.34 ± 1.22^{B}
ANOVA	Priming treatments (PT)	***	***	***	***	***	**	***
	Manganese toxicity (Mn)	***	***	***	***	***	***	***
	PT × Mn	**	***	ns	**	**	ns	**

750 mg kg^{-1}Mn levels, respectively. Coumarin (50 and 100 mg L^{-1}) substantially decreased (14.26 and 16.12% under 450 mg kg^{-1} Mn; 22.41 and 20.16% under 750 mg kg^{-1} Mn, respectively) H_2O_2 levels relative to unprimed plants (Table 5).

Manganese stress (450 and 750 mg kg^{-1}) displayed clear signs of oxidative injury in the form of over-production (155.8 and 338.23%, respectively) of $O_2^{\bullet-}$. The production of $O_2^{\bullet-}$ was concentration-dependent as higher Mn levels induced maximal $O_2^{\bullet-}$ generation. Exogenous COU (50 and 100 mg L^{-1}) considerably assuaged (30.76 and 35.91% under 450 mg kg^{-1} Mn; 33.72 and 38.05% mg kg^{-1} Mn, respectively) $O_2^{\bullet-}$ generation compared with unprimed plants (Table 5).

Our results revealed a drastic increase (88.75 and 194.12%) in lipoxygenase activity (LOX) under 450 and 750 mg kg^{-1} Mn levels, respectively. Exogenous COU (50 and 100 mg L^{-1}) induced a noteworthy depression (37.55 and 21.97% under 450 mg kg^{-1} Mn; 24.12 and 26.6% under 750 mg kg^{-1} Mn, respectively) in LOX activity relative to control plants (Table 5).

Exposure of sesame plants to Mn toxicity (450 and 750 mg kg^{-1}) led to a significant increase (67.36 and 287.59%, respectively) in oxidized glutathione (GSSG) levels. Further, exogenous COU (50 and 100 mg L^{-1}) caused a considerable decline (50.2 and 28.51% under 450 mg kg^{-1} Mn; 23.54 and 17.13% under 750 mg kg^{-1} Mn, respectively) in GSSG levels relative to unprimed plants (Fig. 2).

3.11 Leaf relative water content (LRWC) and osmolyte accumulation

Leaf relative water content (LRWC) diminished significantly (20.93 and 32.97%) in sesame plants under Mn 450 and 750 mg kg^{-1} levels, respectively. Coumarin (50 and 100 mg L^{-1}) notably improved LRWC values (12.74 and 10.57% under 450 mg kg^{-1} Mn; 27.03 and 21.11% under 750 mg kg^{-1} Mn, respectively) relative to unprimed plants (Table 5).

Manganese toxicity (450 and 750 mg kg^{-1} Mn) significantly enhanced (21.4 and 56.9%, respectively) glycine betaine (GB) contents of sesame plants. Exogenous COU (50, and 100 mg L^{-1}) demonstrated a more conspicuous upsurge (30.83 and 28.89% under 450 mg kg^{-1} Mn; 18.92 and 25.39% under 750 mg kg^{-1} Mn, respectively) in GB values relative to control plants (Table 5).

Proline accumulation notably increased (23.81 and 83.98%) in plants under 450 and 750 mg kg^{-1} Mn levels, respectively. Further, COU administration, especially 50 and 150 mg L^{-1}, effectively improved (34.89 and 32.86% under 450 mg kg^{-1} Mn, respectively) proline levels and COU (100 and 150 mg L^{-1}) manifested upsurge in proline content (12.99 and 13.71%, respectively) under 750 mg kg^{-1}Mn as compared to control plants (Table 6).

3.12 Endogenous nitric oxide (NO) content

Endogenous nitric oxide (NO) levels increased notably (55.45 and 87.9%) in sesame plants after exposure to 450 and 750 mg kg^{-1} Mn levels, respectively. Exogenous COU (50 and 100 mg L^{-1}) considerably improved NO levels (52.56 and 40.79% under 450 mg kg^{-1} Mn; 86.49 and 50.07% under 750 mg kg^{-1} Mn, respectively) compared with control plants (Table 6).

3.13 *Hydrogen sulphide (H_2S) levels*

The amount of H_2S increased (20.22 and 38%) by many folds in sesame plants under 450 and 750 mg kg^{-1} Mn toxicity, respectively. Besides, COU (50 and 100 mg L^{-1}) seed priming resulted in a substantial rise in H_2S levels (32.06 and 34.46% under 450 mg kg^{-1} Mn; 35.11 and 6.16% under 750 mg kg^{-1} Mn, respectively) relative to control plants (Table 6).

3.14 *Histochemical detection of $O_2^{\bullet-}$ and H_2O_2*

Manganese toxicity induced significant oxidative stress in sesame plants by producing $O_2^{\bullet-}$ and H_2O_2. Histochemical staining revealed large brown spots representing H_2O_2, while dark blue staining reflected $O_2^{\bullet-}$ production in leaves of Mn-stressed plants. Conversely, COU-administered seedlings manifested lesser $O_2^{\bullet-}$ and H_2O_2 on leaf surface under Mn toxicity (Figure S6 & S7; Appendix-III).

3.15 Antioxidant enzymes

A significant increase (16.48 and 38.12%) in superoxide dismutase (SOD) activity was observed in plants under 450 and 750 mg kg^{-1} Mn, respectively. Besides, COU administration (50, 100, and 150 mg L^{-1}) notably raised (54.46, 46.68 and 26.46% under 450 mg kg^{-1} Mn; 65.34, 49.52 and 19.08% under 750 mg kg^{-1} Mn, respectively) SOD activity compared with unprimed plants (Table 6).

Manganese stress (450 and 750 mg kg^{-1} Mn) resulted in a substantial increase (13.65 and 48.54%, respectively) in peroxidase (POD) activity in sesame plants. The increase in POD activity was more substantial (122.52 and 96.24% under 450 mg kg^{-1} Mn; 67.53 and 44.89% under 750 mg kg^{-1} Mn) by COU priming, particularly in plants fed with 50 and 100 mg L^{-1}, respectively (Table 6).

Catalase activity (CAT) increased by several folds (24.07 and 69.45%) in sesame plants after exposure to 450 and 750 mg kg^{-1} Mn, respectively. A COU-mediated rise in CAT activity (94.09, 79.56 and 42.32% under 450 mg kg^{-1} Mn; 95.63, 92.99 and 71.77% under 750 mg kg^{-1} Mn) was evident in plants treated with 50, 100 and 150 mg L^{-1} COU respectively, over control plants (Table 6).

Table 6 Effect of exogenous coumarin on proline, hydrogen sulphide (H_2S), nitric oxide (NO), nitrate reductase activity (NRA), superoxide dismutase activity (SOD), peroxidase activity (POD), and catalase activity (CAT) in sesame (*Sesamum indicum* L.) under Mn toxicity. Data are means ± standard error of four replicates ($n = 4$). The values in each column followed by different letters are significantly different at 95% confidence level according to least significant difference (LSD) test. ** reflects $P \leq 0.01$; *** reflects $P \leq 0.001$; ns reflects non-significant

Source of variations		Proline (μmol g^{-1} FW)	H_2S (μmol g^{-1} FW)	NO (nmol g^{-1} FW)	NRA (μmol NO_2 h^{-1} g^{-1} FW)	SOD (Units mg^{-1} protein)	POD (Units mg^{-1} protein)	CAT (Units mg^{-1} protein)
Mn 0 mg kg^{-1} soil	Unprimed	3.45 ± 0.20^{FGH}	9.66 ± 0.28^{G}	10.59 ± 0.56^{H}	25.60 ± 1.06^{CDE}	21.67 ± 0.63^{GH}	7.23 ± 0.51^{CD}	13.18 ± 0.54^{G}
	Hydro-primed	2.54 ± 0.43^{GH}	10.43 ± 0.27^{FG}	10.28 ± 1.84^{H}	26.16 ± 0.78^{CD}	21.98 ± 0.27^{Gh}	7.32 ± 0.20^{CD}	14.97 ± 2.60^{G}
	COU 50 mg L^{-1}	2.41 ± 0.43^{H}	11.78 ± 1.49^{CDEFG}	9.94 ± 1.20^{H}	25.39 ± 2.43^{CDE}	20.62 ± 0.88^{GH}	9.38 ± 0.38^{BC}	27.50 ± 2.64^{BCD}
	COU 100 mg L^{-1}	3.72 ± 0.43^{EFG}	10.84 ± 0.56^{EFG}	8.65 ± 0.26^{H}	32.89 ± 4.10^{AB}	22.22 ± 1.58^{Gh}	9.08 ± 0.30^{BC}	21.99 ± 2.21^{DEF}
	COU 150 mg L^{-1}	4.86 ± 0.32^{CDE}	9.66 ± 0.28^{G}	9.90 ± 1.11^{H}	30.45 ± 1.20^{ABC}	17.74 ± 1.68^{H}	5.33 ± 0.20^{D}	18.86 ± 2.81^{EFG}
Mn 450 mg kg^{-1} soil	Unprimed	4.28 ± 0.40^{DEF}	11.62 ± 1.09^{DEFG}	16.46 ± 0.37^{G}	23.17 ± 2.17^{DEF}	25.24 ± 1.69^{FG}	8.21 ± 0.62^{BCD}	16.35 ± 0.52^{FG}
	Hydro-primed	4.24 ± 0.24^{EF}	12.53 ± 1.21^{CDEF}	18.40 ± 0.29^{FG}	25.55 ± 0.95^{CDE}	25.34 ± 2.15^{FG}	9.98 ± 1.06^{BC}	18.72 ± 2.16^{EFG}
	COU 50 mg L^{-1}	5.77 ± 0.34^{BC}	15.34 ± 1.01^{B}	25.13 ± 1.36^{BCD}	33.92 ± 3.22^{A}	38.99 ± 2.83^{B}	18.27 ± 1.69^{A}	31.86 ± 3.16^{B}
	COU 100 mg L^{-1}	5.44 ± 0.41^{BCD}	15.62 ± 1.25^{AB}	23.19 ± 2.004^{CDE}	31.01 ± 2.29^{ABC}	37.03 ± 2.64^{BC}	16.11 ± 2.04^{A}	29.36 ± 3.03^{BC}
	COU 150 mg L^{-1}	5.68 ± 0.37^{BC}	13.82 ± 0.62^{BCD}	16.03 ± 0.58^{G}	27.13 ± 1.38^{BCD}	31.92 ± 3.42^{DE}	8.11 ± 1.11^{BCD}	23.26 ± 1.66^{CDE}
Mn 750 mg kg^{-1} soil	Unprimed	6.35 ± 0.80^{AB}	13.33 ± 1.40^{BCDE}	19.90 ± 0.29^{EFG}	18.47 ± 2.56^{F}	29.93 ± 0.46^{EF}	10.73 ± 1.11^{B}	22.32 ± 1.01^{DEF}
	Hydro-primed	6.25 ± 0.49^{AB}	12.67 ± 0.90^{CDEF}	21.88 ± 4.12^{DEF}	19.97 ± 3.14^{EF}	33.44 ± 0.65^{CDE}	9.61 ± 1.58^{BC}	24.47 ± 0.76^{CDE}
	COU 50 mg L^{-1}	5.80 ± 0.83^{BC}	18.01 ± 1.13^{A}	37.13 ± 3.66^{A}	28.29 ± 2.82^{ABCD}	49.49 ± 2.23^{A}	17.98 ± 1.61^{A}	43.68 ± 4.37^{A}
	COU 100 mg L^{-1}	7.17 ± 0.66^{A}	14.15 ± 1.16^{BC}	29.88 ± 3.20^{B}	29.33 ± 1.92^{ABC}	44.75 ± 2.90^{A}	15.55 ± 2.10^{A}	43.10 ± 3.38^{A}
	COU150 mg L^{-1}	7.22 ± 0.26^{A}	11.24 ± 1.35^{EFG}	27.15 ± 1.52^{BC}	27.38 ± 2.31^{BCD}	35.64 ± 2.91^{BCD}	10.23 ± 1.23^{BC}	38.35 ± 3.52^{A}
ANOVA	Priming treatments (PT)	***	***	***	***	***	***	***
	Manganese toxicity (Mn)	***	***	***	**	***	***	***
	PT × Mn	ns	ns	***	ns	***	**	ns

3.16 Methylglyoxal toxicity and glyoxalase system

Manganese toxicity notably disrupted methylglyoxal (MG) detoxification in sesame plants. The activities of enzymes of the glyoxalase system (Gly I and Gly II) decreased substantially (Gly I: 13.96 and 56.12%; Gly II: 25.25 and 44.4%) in plants upon exposure to 450 and 750 mg kg^{-1} Mn levels, respectively. Lower Gly I and Gly II enzyme activities alongside higher MG levels (258.7 and 396%) were evident in plants subjected to Mn stress (450 and 750 mg kg^{-1}). Besides, COU (50 and 100 mg L^{-1}) priming markedly reduced (28.77 and 12.18% under 450 mg kg^{-1} Mn; 19.53 and 15.46% under 750 mg kg^{-1} Mn, respectively) MG levels by strengthening the activities of Gly I (36.36 and 23.37% under 450 mg kg^{-1} Mn; 32.42 and 23.5% under 750 mg kg^{-1} Mn, respectively) and Gly II (35.13 and 45.94% under 450 mg kg^{-1} Mn; 10.9 and 25.45% under 750 mg kg^{-1} Mn, respectively) enzymes relative to unprimed plants (Fig. 1).

3.17 Ascorbate–glutathione cycle (AsA-GSH) enzymes

Activities of the ascorbate–glutathione (AsA-GSH) cycle enzymes, namely APX (44.63 and 76.85%), MDHAR (59.51 and 121.75%), DHAR (24.26 and 64.36%), and GR (61.67 and 131.29%), increased significantly in sesame plants upon exposure to 450 and 750 mg kg^{-1} Mn levels, respectively. Higher activities of ASA-GSH cycle enzymes occurred in plants under higher Mn levels. Exogenous COU (50 and 100 mg L^{-1}) enhanced APX (37.45 and 50.9%; 49.17 and 69%), MDHAR (31.87 and 36.17; 29.35 and 31.39%), DHAR (65.23 and 41.44%; 32.03 and 28.93%) and GR

enzyme activities (49.63 and 27.15% under 450 mg kg^{-1} Mn; 40.52 and 33.11% under 750 mg kg^{-1} Mn), respectively relative to unprimed plants (Fig. 2).

3.18 Thiol-dependent antioxidant enzyme

Our results revealed a significant increase (52.05 and 176.7%) in the activity of glutathione *S*-transferase (GST), an important thiol-dependent antioxidant enzyme, under 450 and 750 mg kg^{-1} Mn levels. Further, COU (50 and 100 mg L^{-1}) induced a noteworthy improvement (46.88 and 62.27% under 450 mg kg^{-1} Mn; 41.47 and 30.32% under 750 mg kg^{-1} Mn, respectively) in the activity of GST over control plants (Fig. 2).

3.19 Nutrient acquisition

Sesame plants manifested a significant drop in root (36.1 and 55.19%) and leaf (42.66 and 61.62%) K content under

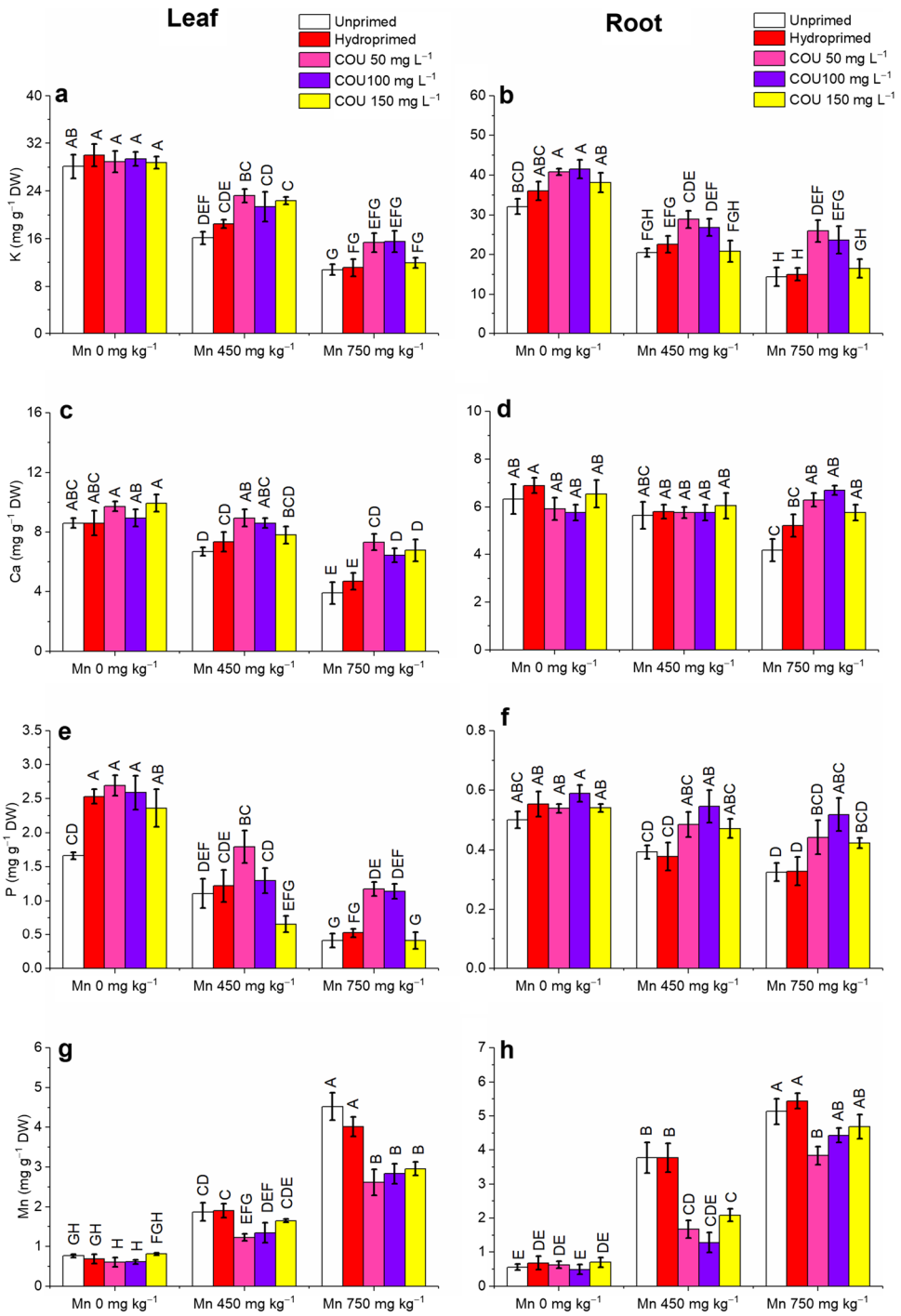

Fig. 3 Coumarin-mediated nutrient acquisition in sesame (*Sesamum indicum* L.) under Mn toxicity. Uppercase letters on standard error bars represent significance among treatments at 95% confidence level

450 and 750 mg kg^{-1} Mn, respectively. Further, COU (50 and 100 mg L^{-1}) notably enhanced K levels in root (40.65 and 30.89% under 450 mg kg^{-1} Mn; 80.28 and 64.63% under750 mg kg^{-1} Mn, respectively) and leaf (43.92 and 32.29% under 450 mg kg^{-1} Mn; 42.08 and 43.62% under 750 mg kg^{-1} Mn, respectively) relative to control plants (Fig. 3). Likewise, a significant fall in leaf Ca (22.10 and 54.48%) and root Ca levels (10.79 and 33.97%) were apparent in plants under 450 and 750 mg kg^{-1}, respectively. Exogenous COU (50, 100, and 150 mg L^{-1}) induced a noticeable improvement in leaf Ca levels (33.6, 28.37 and 16.67% under 450 mg kg^{-1} Mn; 87.34, 64.76 and 73.28% under 750 mg kg^{-1} Mn, respectively) over unprimed plants, while COU priming did not affect root Ca contents (Fig. 3). Likewise, a notable abridge (29.17 and 37.06%) in leaf nitrogen content was seen in sesame plants exposed to 450 and 750 mg kg^{-1} Mn, respectively. Besides, COU priming (50 and 100 mg L^{-1}) noticeably raised the values (33.16 and 35.2% under 450 mg kg^{-1} Mn; 42.63 and 23.83% under 750 mg kg^{-1} Mn, respectively) of nitrogen contents in a comparison to unprimed plants (Figure S10; Appendix-III).

Plants under Mn stress (450 and 750 mg kg^{-1} Mn) exhibited a significant fall in leaf (33.3 and 75.24%, correspondingly) and root P levels (21.41 and 35%, correspondingly). Conversely, COU (50 and 100 mg L^{-1}) priming, induced a remarkable improvement in leaf P (61.96 and 17.1% under 450 mg kg^{-1} Mn; 184.59 and 176.98% under 750 mg kg^{-1} Mn, respectively) and root P (23.39 and 38.7% under 450 mg kg^{-1} Mn; 35.9 and 59.49% under 750 mg kg^{-1} Mn, correspondingly) levels relative to control plants (Fig. 3).

Manganese toxicity (450 and 750 mg kg^{-1} Mn) led to a more significant Mn accumulation in roots (572 and 814.65%, respectively) and leaves (145.25 and 493.14%, respectively). Further COU (50 and 100 mg L^{-1}) diminished root Mn (55.5 and 65.94% under 450 mg kg^{-1} Mn; 25.13 and 13.57% under 750 mg kg^{-1} Mn, correspondingly) and leaves (34.45 and 28.19% under 450 mg kg^{-1} Mn; 42.14 and 37.4% under 750 mg kg^{-1} Mn, respectively) compared to unprimed plants. Likewise, COU seed priming also limited the aerial translocation of Mn, thereby protecting plants from phytotoxic effects of Mn toxicity (Figure S10; Appendix-III).

Manganese toxicity (450 and 750 mg kg^{-1} Mn) led to a significant fall in root Zn (230.7 and 173%, respectively) and leaf Zn (67.9 and 56.6%, respectively). Coumarin (50 and 100 mg L^{-1}) increased leaf Zn (220 and 137.89% under 450 mg kg^{-1} Mn; 118.95 and 48.37% under 750 mg kg^{-1} Mn, respectively) and root Zn (146.37 and 67.79% under 450 mg kg^{-1} Mn; 104.4 and 70.72% under 750 mg kg^{-1} Mn, respectively) in sesame plants compared with control plants (Fig. 4).

Magnesium (Mg) levels decreased considerably in roots (45.87 and 86.26%) and leaves (54.35 and 66.55%) of sesame plants upon exposure to 450 and 750 mg kg^{-1} Mn, respectively. In this context, COU (50 and 100 mg L^{-1}) noticeably improved Mg levels in leaves (351.87 and 311.37% under 450 mg kg^{-1} Mn; 506.13 and 402.79% under 750 mg kg^{-1} Mn, respectively) and roots (47.03 and 41.43% under 450 mg kg^{-1} Mn; 211.64 and 160.03% under 750 mg kg^{-1} Mn, respectively) relative to control plants (Fig. 4).

We noticed a considerable abridge in the values of root (20.04 and 46.86%) and leaf Fe (43.99 and 74.65%) in sesame plants upon exposure to 450 and 750 mg kg^{-1} Mn levels, respectively. Besides, COU (50, 100 and 150 mg L^{-1}) significantly enhanced leaf Fe (56.5, 79.49 and 55.57% under 450 mg kg^{-1} Mn; 172.96, 93.41 and 58.04% under 750 mg kg^{-1} Mn, respectively) while COU (50 and 100 mg L^{-1}) exhibited visible rise in root Fe (39.61 and 32.2% under 450 mg kg^{-1} Mn; 81.59 and 49.98% under 750 mg kg^{-1} Mn, respectively) compared with unprimed sesame plants (Fig. 4).

4 Discussion

Manganese toxicity is detrimental for plants; therefore, an acquaintance of Mn phytotoxic effects on plant morphological, physiological and biochemical indices is essential to understanding plant defense responses (Noor et al. 2022). Our results manifested a significant depression in different growth attributes in sesame plants under Mn stress. The diminished growth attributes are the consequences of Mn interference with crucial metabolic processes, including photosynthesis, chlorophyll contents, protein synthesis, enzyme activities, and damage to critical cellular compartments (Berríos et al. 2019). Our results also revealed a significant fall in photosynthesis rate, chlorophyll contents, acquisition of essential nutrients alongside a substantial rise in the uptake and accumulation of Mn in aerial plant parts. Coumarin significantly improved plant growth attributes under Mn toxicity. Coumarin-mediated bettered plant growth under Mn toxicity is ascribed to minimal chlorophyll degradation, improved photosynthesis, and nutrient acquisition. Also, plants administered coumarin accumulated lesser Mn contents under Mn toxicity. In this context, Santos et al. (2017) reported that plants accumulating lower Mn had better growth under Mn toxicity in soybean. Likewise, Najeeb et al. (2009) also documented minimal growth in plants stressed with higher Mn dose in *Juncus effusus* L. Oxidative injury also negatively affected plant growth under Mn toxicity (Fan et al. 2020). Our results manifested a negative correlation of shoot fresh and dry

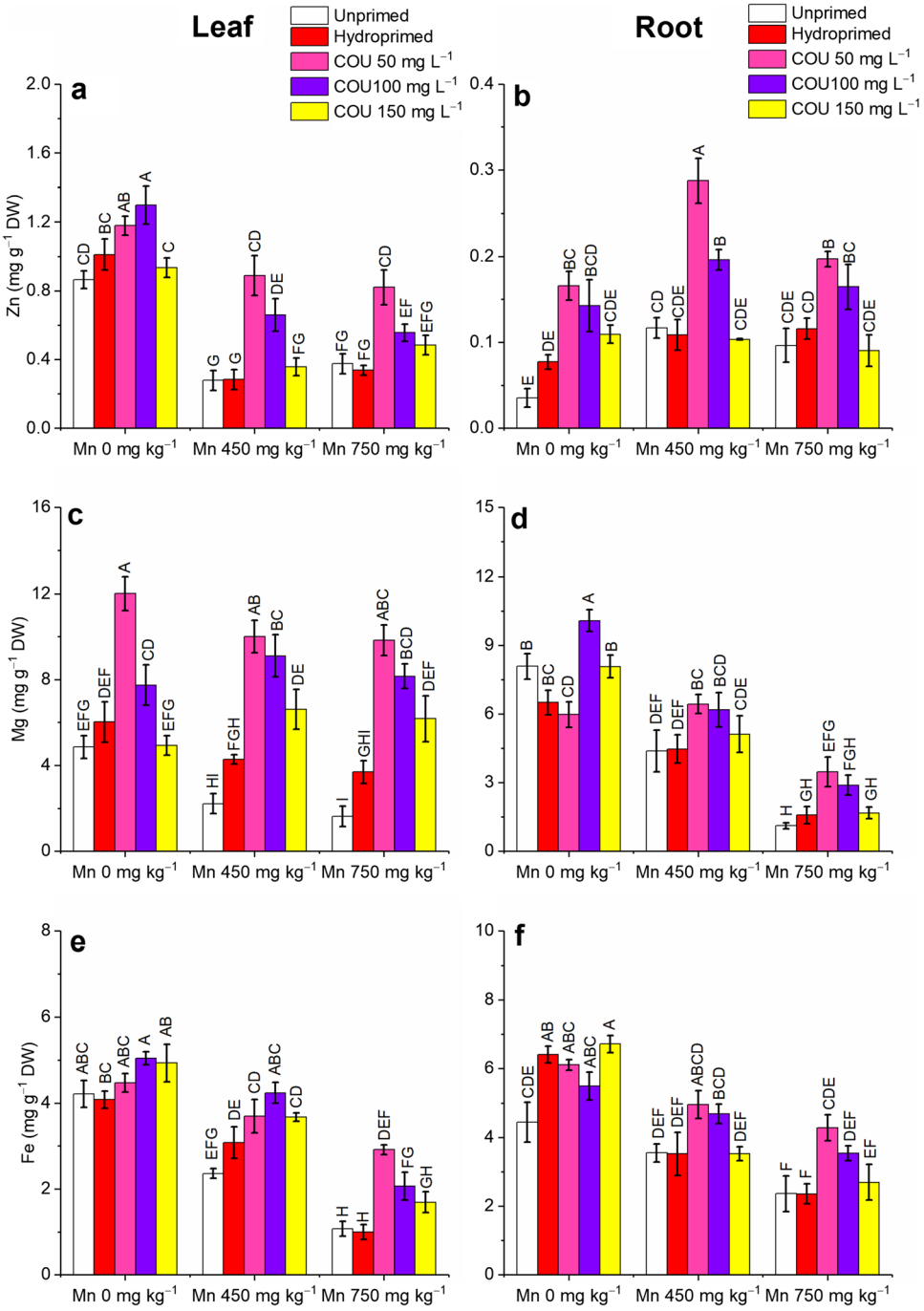

Fig. 4 Coumarin-mediated nutrient acquisition in sesame (*Sesamum indicum* L.) under Mn toxicity. Uppercase letters on standard error bars represent significance among treatments at 95% confidence level

weight with ROS production, lipid peroxidation, and LOX activity (Figure S9; Appendix-III). The schematic representation of COU-mediated tolerance to Mn toxicity in sesame is represented in Fig. 5.

Changes in photosynthetic pigments have direct influence on photosynthesis rates in plants (Yang et al. 2022). Manganese toxicity reduces Mg and Fe contents of plants that in turn lessens chlorophyll contents. Oxidative injury due to excessive ROS generation also causes fall in chlorophyll contents (Ahmad et al. 2022). Our results also revealed significantly diminished Mg and Fe levels under Mn toxicity. Further, we noticed a significant upsurge in oxidative damage due to enhanced ROS generation that might have degraded chlorophyll pigment. Our findings revealed that oxidative stress markers held a strong negative correlation with shoot fresh and dry weights (Figure S9; Appendix-III).

Manganese toxicity impedes electron transfer between the two photosystems and thereby reduces photosynthesis in plants. Further, significant damage in photosynthetic pigments also result in poor CO_2 assimilation rate (Hussain

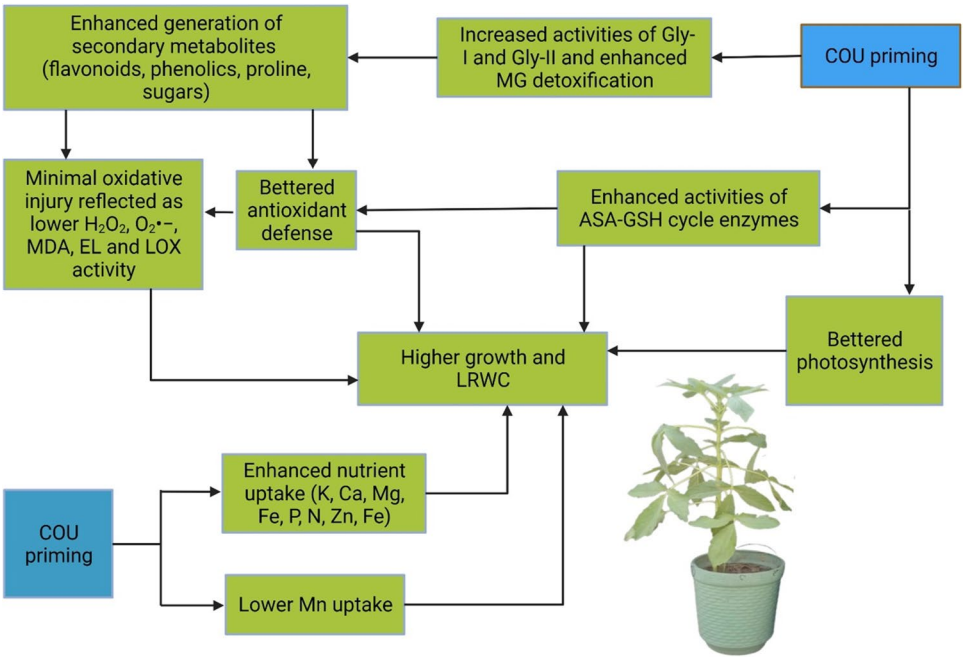

Fig. 5 Mechanistic representation of coumarin-mediated Mn tolerance in sesame plants

et al. 2019; Li et al. 2010). Mn toxicity also induced a significant fall in stomatal conductance values. In agreement with our results, Berríos et al. (2019) reported diminished stomatal conductance and transpiration rate in ryegrass under Mn toxicity. Hussain et al. (2019) also found a significant decline in stomatal conductance and transpiration rate in *Brassica juncea* under Mn toxicity. Plants close their stomata as an adaptive strategy to restrict the aerial translocation of Mn from roots (Hussain et al. 2019). The photosynthetic potential of sesame plants is also limited due to Mn-induced oxidative damage. The deterioration of photosynthetic apparatus also decreases water use efficiency in plants, as evident in our study (Rojas-Lillo et al. 2014). Coumarin improved photosynthesis, stomatal conductance, transpiration rate and water use efficiency in sesame plants under Mn toxicity. Oxidative damage causes a remarkable reduction in photosynthesis and other gas exchange attributes in plants under Mn toxicity (Noor et al. 2022). We also noticed a negative association of oxidative stress markers (H_2O_2, $O_2^{\bullet-}$, LOX activity, EL, and MDA) with photosynthesis in sesame plants under Mn toxicity.

Disturbances in plant water relations are common effects of metal toxicity (Mostofa and Fujita 2013). Our results manifested a significant drop in LRWC of sesame plants under Mn toxicity. In agreement with our study, Sheng et al. (2016) reported a decline in LRWC in wheat plants under Mn toxicity. Further, metal toxicity induces osmotic stress that might diminish LRWC (Mostofa and Fujita 2013). Oxidative damage also causes substantial reduction in water status of plants under Mn toxicity (Noor et al. 2022). In our study, decline in LRWC due to oxidative damage is validated from Figure S9 (Appendix-III) which indicated a significant negative correlation of oxidative stress markers with LRWC. Coumarin significantly decreased oxidative injury that might have enhanced LRWC in sesame plants under Mn toxicity.

Soluble sugars interact with membrane components and safeguard them from ROS (Valivand and Amooaghaie 2021). Plants grown under stressful conditions show significant suppression in growth and photosynthesis, resulting in soluble carbohydrates that wage metabolic adjustments to maintain cell turgor and stabilize cell membranes (Keunen et al. 2013). Our results exhibited a notable improvement in soluble sugars accumulation in plants administered COU under Mn toxicity. Therefore, the influence of COU on improved LRWC is due to a COU-mediated increase in soluble sugars that work as osmoticum in Mn-stressed plants (Valivand and Amooaghaie 2021).

The increase in the accumulation of free amino acids indicates better metal tolerance due to their functions in metal binding besides their role as osmolytes (Khan et al. 2020). Amino acids are the precursors of phytohormones and the reservoirs of proteins that aid plants in tolerating oxidative injury better (Ulhassan et al. 2019). Our studies revealed a significant improvement in free amino acids accumulation in sesame plants pre-treated with COU under Mn stress.

The upsurge in total soluble proteins could be due to efficient gas exchange and photosystems regulated by COU administration in plants under Mn toxicity (Mukta et al. 2019). In our study, COU supplementation improved photosynthetic efficiency by maintaining higher sugars and proteins that could circumvent the harmful effects of Mn stress. Glycine betaine (GB) and proline accumulation in plants safeguard major cellular

compartments alongside maintaining cell turgor (Anjum et al. 2017). Increased osmolyte accumulation may guard enzymatic activity by scavenging ROS (Qureshi et al. 2020). Higher GB and proline accumulation lead to better photosynthesis and plants' growth under stressful conditions (Ahmad et al. 2018). Coumarin increased GB and proline levels that might have improved growth, LRWC, photosynthesis, and reduced oxidative damage (Farouk and Al-Amri 2019).

Nitric oxide (NO) mediates plant defense responses to several environmental constraints (Okant and Kaya 2019), but the studies on NO metabolism under Mn toxicity are scarce. A significant increase in NRA activity with a concurrent rise in NO levels occurred in sesame plants pre-treated with COU under Mn toxicity. Nitrate reductase (NRA) is an essential enzyme in the nitrogen assimilation pathway with a significant capacity to reduce (nitrite) NO_2^- to nitric oxide (NO). Metal toxicity also generates osmotic stress as a secondary effect that might have suppressed NRA activity with an accompanying fall in NO levels (Mostofa and Fujita 2013; Hayat et al. 2012). The lower endogenous levels for NO weakened the oxidative defense system under stress, as evident in our results (Khan et al. 2017).

Our results manifested a significant rise in H_2S levels in plants supplemented with COU under Mn toxicity (Table 3). H_2S significantly diminishes the uptake and accumulation of metals and improves plant tolerance to metals. Further, H_2S also scavenges ROS because it is a reductive substance (He et al. 2018).

Our findings also demonstrated the existence of oxidative damage reflected as higher MDA, H_2O_2, $O_2^{\bullet-}$, and EL levels alongside strengthened LOX activity in sesame plants under Mn toxicity. Our results are in corroboration with the findings of Parashar et al. (2014) in Mn-stressed *Brassica juncea* plants. Likewise, GSSG levels increased remarkably, and GSH:GSSG ratio dropped sharply under metal toxicity (Ahmad et al. 2021). Our results also demonstrated a noticeable fall in GSH values and GSH:GSSG ratio in sesame plants under Mn toxicity. Mn-stressed plants failed to maintain GR activity; this is why the GSH levels were not adequate to uphold a higher GSH:GSSG ratio to diminish ROS generation and oxidative injury. The results are in agreement with the earlier reports on rice, rapeseed under salinity (Alam et al. 2013; Rahman et al. 2016), and tomato under chromium toxicity (Alamri et al. 2020). Plants need a precise equilibrium between GSH and GSSG to maintain cellular redox balance (Hasanuzzaman et al. 2018a). Noor et al. (2022) reported the decline in GSH and GSH:GSSG ratio that generated noteworthy oxidative damage in *Prunus persica* plants.

Sesame plants displayed a significant fall in DPPH activity under Mn toxicity. However, COU remarkably improved the total antioxidant potential of plants, reflected in higher DPPH activity. Plant exposed to metal toxicity exhibit diminished DPPH activities as reported in rice (Tripathi et al. 2012), *Ricinus communis* (Qureshi et al. 2020), and red bean Mahdavian (2021).

The antioxidant defense system counteracts ROS generated in plants under manganese toxicity (Berríos et al. 2019). Plants produce ASA and GSH (non-enzymatic antioxidants) to neutralize ROS effects and maintain cellular redox status (Kaya et al. 2020). Our results depicted a significant fall in GSH and ASA (reduced forms). In contrast, a substantial increase in GSSG (oxidized forms of GSH) was evident in plants under Mn toxicity. The redox potential of GSH and ASA play a critical part in strengthening the oxidative defense in plants.

Glutathione works as a chelator to detoxify heavy metals. It also activates glutathione-*S*-transferase activity to safeguard membranes against the detrimental outcomes of substances generated in response to the oxidation of proteins and lipids (Hasanuzzaman et al. 2017). Further, the outcomes of the present study also revealed remarkable alterations in the cellular redox status mirrored as disturbed ASA and GSH pools in sesame plants under Mn toxicity. Kaya et al. (2020) reported similar modifications in cellular redox status by disturbances in GSH and ASA pools in pepper plants under boron toxicity. However, COU noticeably restored the redox potential of GSH and ASA pools reflected as enhanced ASA and GSH levels, thereby dropping GSH/GSSG. The GSH:GSSG is more crucial in the defense response for ROS detoxification than GSH or ASA levels alone (Hasanuzzaman et al. 2019). In our study, COU remarkably improved GSH:GSSG in sesame plants under Mn toxicity. Higher GSH:GSSG ratio significantly determines plant metal tolerance ability diminishing oxidative injury in plants. Our findings are in corroboration with previous reports in *Brassica napus* under drought (Hasanuzzaman et al. 2018a) and cadmium toxicity (Hasanuzzaman et al. 2018b).

The increased flavonoids and phenolics in sesame plants neutralize ROS effects and form complexes with metals by chelation to reduce phytotoxic effects (Handa et al. 2018). Coumarin significantly enhanced the endogenous levels of phenolics and flavonoids that could further improve plant metal tolerance potential.

Our results displayed significant alterations in the activities of enzymes of ASA-GSH pathway, such as MDHAR, DHAR, GR, and APX in Mn-stressed sesame plants. Similar findings are reported by Mahmud et al. (2017) in canola under chromium toxicity. However, COU remarkably assuaged the detrimental effects of Mn toxicity on growth characteristics and chlorophyll by diminishing ROS generation, oxidative injury, and strengthening the activities of enzymes of ASA-GSH cycle.

APX is the key enzyme of ASA-GSH cycle consuming ASA as electron donor to scavenge H_2O_2 to water (Hasanuzzaman et al. 2019). Our results indicated a significant upsurge in APX activities of sesame plants under Mn toxicity. Similar findings are reported in pepper (Kaya et al. 2020), wheat

(Yildiztugay et al. 2019), and lettuce (Sahin et al. 2017). In our study, COU significantly improved APX activity of sesame plants under Mn toxicity. Glutathione reductase (GR) is also an essential enzyme of ASA-GSH cycle, which enhances ROS detoxification to undermine oxidative injury (Biju et al. 2021). Our findings revealed a significant increase in the activity of GR in sesame plants under Mn toxicity. Kaya et al. (2020) also reported a substantial increase in GR activity of pepper plants under boron toxicity. However, Mn toxicity mediated rise in GR activity may not be sufficient to uphold higher GSH:GSSG and diminish oxidative injury. Coumarin notably enhanced GR activity and also maintained a higher GSH:GSSG ratio, thereby significantly subsiding oxidative damage in sesame plants.

Other enzymes involved in ASA-GSH cycle are DHAR and MDHAR. The conversion of oxidized ascorbate to reduced ascorbate is catalyzed by DHAR enzyme, while MDHAR enzyme participates in restoring the redox status by maintaining reduced ASA pool and higher ASA/DHA (Hasanuzzaman et al. 2019). In the present study, Mn toxicity significantly enhanced the activities of MDHAR and DHAR in sesame plants. However, the rise in MDHAR and DHAR activities in Mn-stressed plants could be due to a fall in GSH contents utilized in phytochelatin synthesis. The higher demand for GSH is provided through enhanced DHAR, MDHAR, and GR activities. Further, our findings suggested the central role of GR, DHAR, and MDHAR activities in defense against Mn toxicity. Similar results were also reported by Mishra et al. (2022) in rice.

Further, activities of antioxidant enzymes SOD, POD, and CAT notably increased in sesame plants under Mn toxicity. The rise in activities of antioxidant enzymes (SOD, POD, and CAT) has been reported previously in pepper under boron toxicity (Kaya et al. 2020). Coumarin significantly strengthened the activities of antioxidant enzymes reflected as minimal oxidative injury in plants.

Methylglyoxal is generated due to regular respiration-associated metabolic events, and its production is several folds higher in plants under stress (Hasanuzzaman et al. 2018b). Mn toxicity in sesame plants induced a significant rise in MG levels alongside a notable fall in the activities of MG detoxification enzymes Gly I and Gly II. Coumarin administration considerably enhanced Gly I and Gly II enzyme activities and the levels of GSH, which is a cofactor in the MG detoxification reaction. Consequently, plants pre-treated with COU manifested lesser MG production under Mn toxicity.

The reports concerning the effects of exogenous COU on nutrient acquisition in plants under Mn toxicity are scarce. The present study reveals a significant improvement in the nutrient acquisition of plants pretreated with COU under Mn toxicity. Our results manifested a notable fall in K, Ca, P, Zn, Mg, and Fe levels alongside higher Mn levels in plants under Mn toxicity. The metals bear structural resemblances with crucial nutrients (K, Ca, Fe, Mg, and Zn), and thereby, the excess metals can interfere with the uptake and translocation of nutrients (Rasheed et al. 2018; Ulhassan et al. 2019; Qureshi et al. 2020). Coumarin substantially enhanced plant nutrient acquisition under Mn toxicity. Coumarin diminished oxidative injury that might have bettered nutrient contents in sesame plants under Mn toxicity.

5 Conclusion

Manganese toxicity caused oxidative stress in sesame plants by deteriorating photosynthetic apparatus, degrading chlorophyll molecules, increasing ROS production and lipid peroxidation, and weakening the antioxidant defense system. Our results suggested that COU improved growth, photosynthesis, and nutrient acquisition in plants by regulating ascorbate–glutathione cycle and glyoxalase system under Mn toxicity. Plants pre-treated with COU manifested several folds drop in ROS generation mirrored in histochemical results under Mn toxicity. Coumarin limited the aerial accumulation of Mn that might have improved the acquisition of other macro-and micronutrients. This study revealed the role of COU in mediating critical physiological and biochemical processes in plants under Mn toxicity. Further, lower COU doses (50 and 100 mg L^{-1}) were effective in strengthening the ascorbate–glutathione cycle and regulating the glyoxalase system for MG detoxification in plants under Mn toxicity.

Supplementary Information The online version contains supplementary material available at https://doi.org/10.1007/s42729-022-00983-w.

Acknowledgements The work reported in this manuscript is part of the Ph.D. dissertation of Mr. Mudassir Iqbal Shad, Reg. No. 2015-GCUF-2115, Ph.D. scholar at Government College University Faisalabad, Pakistan.

Author Contributions Mudassir Iqbal Shad Investigation, methodology, visualization; Rizwan Rasheed conceptualization, visualization; Muhammad Arslan Ashraf Writing-original draft, supervision, methodology, funding acquisition; Shafaqat Ali: review & editing, statistical analysis; Iqbal Hussain Methodology, Investigation.

Funding The funds for the present research work were provided by HEC funded project No: 8345/Punjab/ NRPU/R&D/HEC/ 2017.

Data availability The datasets used in this study are available from the corresponding author on reasonable request.

Declarations

Ethics Approval and Consent to Participate Not applicable.

Consent for Publication Not applicable.

Conflict of Interests The authors declare no competing interests.

References

Ahmad P, Ahanger MA, Egamberdieva D, Alam P, Alyemeni MN, Ashraf M (2018) Modification of osmolytes and antioxidant enzymes by 24-epibrassinolide in chickpea seedlings under mercury (Hg) toxicity. J Plant Growth Regul 37(1):309–322

Ahmad P, Raja V, Ashraf M, Wijaya L, Bajguz A, Alyemeni MN (2021) Jasmonic acid (JA) and gibberellic acid (GA3) mitigated Cd-toxicity in chickpea plants through restricted cd uptake and oxidative stress management. Sci Rep 11(1):19768. https://doi.org/10.1038/s41598-021-98753-8

Ahmad S, Mfarrej MFB, El-Esawi MA, Waseem M, Alatawi A, Nafees M, Saleem MH, Rizwan M, Yasmeen T, Anayat A, Ali S (2022) Chromium-resistant Staphylococcus aureus alleviates chromium toxicity by developing synergistic relationships with zinc oxide nanoparticles in wheat. Ecotoxicol Environ Saf 230:113142. https://doi.org/10.1016/j.ecoenv.2021.113142

Alam MM, Hasanuzzaman M, Nahar K, Fujita M (2013) Exogenous salicylic acid ameliorates short-term drought stress in mustard (*Brassica juncea* L.) seedlings by up-regulating the antioxidant defense and glyoxalase system. Aust J Crop Sci 7 (7):1053

Alamri S, Ali HM, Khan MIR, Singh VP, Siddiqui MH (2020) Exogenous nitric oxide requires endogenous hydrogen sulfide to induce the resilience through sulfur assimilation in tomato seedlings under hexavalent chromium toxicity. Plant Physiol Biochem 155:20–34. https://doi.org/10.1016/j.plaphy.2020.07.003

Alejandro S, Höller S, Meier B, Peiter E (2020) Manganese in Plants: From Acquisition to Subcellular Allocation. Front Plant Sci 11:300. https://doi.org/10.3389/fpls.2020.00300

Allen S, Grimshaw H, Parkinson J, Quamby C, Roberts J (1986) In: Moore PD, Chapman SB (eds) Methods in plant ecology. Chemical Analysis, Blackwell Scientific Publication, Oxford, London, pp 285–344

Anjum SA, Ashraf U, Khan I, Tanveer M, Shahid M, Shakoor A, Wang L (2017) Phyto-Toxicity of Chromium in Maize: Oxidative Damage, Osmolyte Accumulation Anti-Oxidative Defense and Chromium Uptake. Pedosphere 27(2):262–273. https://doi.org/10.1016/S1002-0160(17)60315-1

Ashraf MA, Rasheed R, Zafar S, Iqbal M, Saqib ZA (2021) Menadione sodium bisulfite neutralizes chromium phytotoxic effects in okra by regulating cytosolutes, lipid peroxidation, antioxidant system and metal uptake. Int J Phytoremediation 23(7):736–746

Barrs H, Weatherley P (1962) A re-examination of the relative turgidity technique for estimating water deficits in leaves. Aust J Biol Sci 15(3):413–428

Berríos GA, Luengo Escobar A, Alberdi MR, Nunes-Nesi A, Reyes-Díaz MM (2019) Manganese toxicity amelioration by phosphorus supply in contrasting Mn resistant genotypes of ryegrass. Plant Physiol Biochem 144:144–156. https://doi.org/10.1016/j.plaphy.2019.09.034

Biju S, Fuentes S, Gupta D (2021) Silicon modulates nitro-oxidative homeostasis along with the antioxidant metabolism to promote drought stress tolerance in lentil plants. Physiol Plant 172(2):1382–1398. https://doi.org/10.1111/ppl.13437

Bradford N (1976) A rapid and sensitive method for the quantitation microgram quantities of a protein isolated from red cell membranes. Anal Biochem 72(248):e254

Cakmak I, Horst WJ (1991) Effect of aluminium on lipid peroxidation, superoxide dismutase, catalase, and peroxidase activities in root tips of soybean (*Glycine max*). Physiol Plant 83(3):463–468

Chance B, Maehly AC (1955) Assay of catalases and peroxidases. Methods Enzymology, vol 2. Academic Press, Cambridge, pp 764–775. https://doi.org/10.1016/S0076-6879(55)02300-8

Costa GB, Simioni C, Ramlov F, Maraschin M, Chow F, Bouzon ZL, Schmidt ÉC (2017) Effects of manganese on the physiology and ultrastructure of *Sargassum cymosum*. Environ Exp Bot 133:24–34. https://doi.org/10.1016/j.envexpbot.2016.09.007

Demidchik V (2015) Mechanisms of oxidative stress in plants: From classical chemistry to cell biology. Environ Exp Bot 109:212–228. https://doi.org/10.1016/j.envexpbot.2014.06.021

Doderer A, Kokkelink I, van der Veen S, Valk BE, Schram A, Douma AC (1992) Purification and characterization of two lipoxygenase isoenzymes from germinating barley. Biochim Biophys Acta (BBA)-Protein Struct Mol Enzymol 1120 (1):97–104

Fan P, Yin J, Zhong G, Wu Z (2020) Ascorbic acid alleviation of manganese-induced toxicity in *Vallisneria natans* (Lour.) Hara. Environ Sci Pollut Res 27:32695–32706

Faria JMS, Teixeira DM, Pinto AP, Brito I, Barrulas P, Alho L, Carvalho M (2020) Toxic levels of manganese in an acidic Cambisol alters antioxidant enzymes activity, element uptake and subcellular distribution in *Triticum aestivum*. Ecotoxicol Environ Saf 193:110355. https://doi.org/10.1016/j.ecoenv.2020.110355

Farouk S, Al-Amri SM (2019) Ameliorative roles of melatonin and/or zeolite on chromium-induced leaf senescence in marjoram plants by activating antioxidant defense, osmolyte accumulation, and ultrastructural modification. Ind Crops Prod 142:111823. https://doi.org/10.1016/j.indcrop.2019.111823

Gardner FP, Pearce RB, Mitchell RL (1985) Physiology of crop plants. Iowa State University Press, Ames, USA

Giannopolitis CN, Ries SK (1977) Superoxide dismutases: I Occurrence in higher plants. Plant Physiol 59(2):309–314

Habiba U, Ali S, Rizwan M, Ibrahim M, Hussain A, Shahid MR, Alamri SA, Alyemeni MN, Ahmad P (2019) Alleviative role of exogenously applied mannitol in maize cultivars differing in chromium stress tolerance. Environ Sci Pollut Res 26(5):5111–5121

Hafez AA, Mikkelsen D (1981) Colorimetric determination of nitrogen for evaluating the nutritional status of rice. Commun Soil Sci Plant Anal 12(1):61–69

Hamilton PB, Van Slyke DD, Lemish S (1943) The gasometric determination of free amino acids in blood filtrates by the ninhydrin-carbon dioxide method. J Biol Chem 150:231–250

Handa N, Kohli SK, Thukral AK, Bhardwaj R, Alyemeni MN, Wijaya L, Ahmad P (2018) Protective role of selenium against chromium stress involving metabolites and essential elements in *Brassica juncea* L. seedlings. 3 Biotech 8 (1):66. https://doi.org/10.1007/s13205-018-1087-4

Hasanuzzaman M, Hossain MA, Fujita M (2011) Nitric oxide modulates antioxidant defense and the methylglyoxal detoxification system and reduces salinity-induced damage of wheat seedlings. Plant Biotechnol Rep 5(4):353–365

Hasanuzzaman M, Nahar K, Anee TI, Fujita M (2017) Exogenous silicon attenuates cadmium-induced oxidative stress in *Brassica napus* L. by modulating AsA-GSH pathway and glyoxalase system. Front Plant Sci 8:1061

Hasanuzzaman M, Nahar K, Rahman A, Inafuku M, Oku H, Fujita M (2018a) Exogenous nitric oxide donor and arginine provide protection against short-term drought stress in wheat seedlings. Physiol Mol Biol Plants 24(6):993–1004

Hasanuzzaman M, Nahar K, Rohman MM, Anee TI, Huang Y, Fujita M (2018b) Exogenous Silicon Protects *Brassica napus* Plants from Salinity-Induced Oxidative Stress Through the Modulation of AsA-GSH Pathway, Thiol-Dependent Antioxidant Enzymes and Glyoxalase Systems. Gesunde Pflanzen 70(4):185–194. https://doi.org/10.1007/s10343-018-0430-3

Hasanuzzaman M, Bhuyan MHMB, Anee TI, Parvin K, Nahar K, Mahmud JA, Fujita M (2019) Regulation of Ascorbate-Glutathione Pathway in Mitigating Oxidative Damage in Plants under Abiotic Stress. Antioxidants 8(9):384

Hasanuzzaman M, Bhuyan M, Zulfiqar F, Raza A, Mohsin SM, Mahmud JA, Fujita M, Fotopoulos V (2020) Reactive oxygen species and antioxidant defense in plants under abiotic stress: revisiting the crucial role of a universal defense regulator. Antioxidants 9(8):681

Hayat S, Yadav S, Wani AS, Irfan M, Alyemini MN, Ahmad A (2012) Impact of sodium nitroprusside on nitrate reductase, proline content, and antioxidant system in tomato under salinity stress. Hortic Environ Biotechnol 53(5):362–367. https://doi.org/10.1007/s13580-012-0481-9

He H, Li Y, He L-F (2018) The central role of hydrogen sulfide in plant responses to toxic metal stress. Ecotoxicol Environ Saf 157:403–408. https://doi.org/10.1016/j.ecoenv.2018.03.060

Hossain MA, Nakano Y, Asada K (1984) Monodehydroascorbate reductase in spinach chloroplasts and its participation in regeneration of ascorbate for scavenging hydrogen peroxide. Plant Cell Physiol 25(3):385–395

Hussain A, Nazir F, Fariduddin Q (2019) Polyamines (spermidine and putrescine) mitigate the adverse effects of manganese induced toxicity through improved antioxidant system and photosynthetic attributes in *Brassica juncea*. Chemosphere 236:124830. https://doi.org/10.1016/j.chemosphere.2019.124830

Jackson ML (1969) Soil chemical analysis: advanced course. Soil Science Society of America, Madison, p 894

Jensen A (1978) Chlorophylls and carotenoids. In: Hellebust JA, Craigie JS (eds) Handbook of phycological methods, physiological and biochemical methods. Cambridge University Press, Cambridge, pp 59–70

Joyia FA, Ashraf MY, Shafiq F, Anwar S, Nisa Z-u, Khaliq B, Malik A (2021) Phytotoxic effects of varying concentrations of leather tannery effluents on cotton and brinjal. Agric Water Manag 246:106707. https://doi.org/10.1016/j.agwat.2020.106707

Kaya C, Ashraf M, Al-Huqail AA, Alqahtani MA, Ahmad P (2020) Silicon is dependent on hydrogen sulphide to improve boron toxicity tolerance in pepper plants by regulating the AsA-GSH cycle and glyoxalase system. Chemosphere 257:127241. https://doi.org/10.1016/j.chemosphere.2020.127241

Keunen E, Peshev D, Vangronsveld J, Van Den Ende W, Cuypers A (2013) Plant sugars are crucial players in the oxidative challenge during abiotic stress: extending the traditional concept. Plant Cell Environ 36(7):1242–1255

Khan KY, Ali B, Stoffella PJ, Cui X, Yang X, Guo Y (2020) Study amino acid contents, plant growth variables and cell ultrastructural changes induced by cadmium stress between two contrasting cadmium accumulating cultivars of *Brassica rapa* ssp. chinensis L. (pak choi). Ecotoxicol Environ Saf 200:110748. https://doi.org/10.1016/j.ecoenv.2020.110748

Khan MN, Mobin M, Abbas ZK, Siddiqui MH (2017) Nitric oxide-induced synthesis of hydrogen sulfide alleviates osmotic stress in wheat seedlings through sustaining antioxidant enzymes, osmolyte accumulation and cysteine homeostasis. Nitric Oxide 68:91–102. https://doi.org/10.1016/j.niox.2017.01.001

Kumari S, Khanna RR, Nazir F, Albaqami M, Chhillar H, Wahid I, Khan MIR (2022) Bio-synthesized nanoparticles in developing plant abiotic stress resilience: A new boon for sustainable approach. Int J Mol Sci 23(8):4452

Li Q, Chen L-S, Jiang H-X, Tang N, Yang L-T, Lin Z-H, Li Y, Yang G-H (2010) Effects of manganese-excess on CO2 assimilation, ribulose-1,5-bisphosphate carboxylase/oxygenase, carbohydrates and photosynthetic electron transport of leaves, and antioxidant systems of leaves and roots in *Citrus grandis* seedlings. BMC Plant Biol 10(1):42. https://doi.org/10.1186/1471-2229-10-42

Li P, Song A, Li Z, Fan F, Liang Y (2015) Silicon ameliorates manganese toxicity by regulating both physiological processes and expression of genes associated with photosynthesis in rice (*Oryza sativa* L.). Plant Soil 397 (1–2):289–301

Li Y, Liu K, Zhu J, Jiang Y, Huang Y, Zhou Z, Chen C, Yu F (2019) Manganese accumulation and plant physiology behavior of Camellia oleifera in response to different levels of nitrogen fertilization. Ecotoxicol Environ Safe 184:109603

Lichtenthaler HK (1987) [34] Chlorophylls and carotenoids: pigments of photosynthetic biomembranes. In: Methods Enzymol, Elsevier 148:350–382

Liu Y, Xue Y, Xie B, Zhu S, Lu X, Liang C, Tian J (2020) Complex gene regulation between young and old soybean leaves in responses to manganese toxicity. Plant Physiol Biochem 155:231–242. https://doi.org/10.1016/j.plaphy.2020.07.002

Loomis WE, Shull CA (1937) Methods in plant physiology. McGraw Hill Book Co., New York

Lutts S, Kinet J, Bouharmont J (1995) Changes in plant response to NaCl during development of rice (*Oryza sativa* L.) varieties differing in salinity resistance. J Exp Bot 46 (12):1843–1852

Mahdavian K (2021) Effect of citric acid on antioxidant activity of red bean (*Phaseolus calcaratus* L.) under Cr+6 stress. S Afr J Bot 139:83–91. https://doi.org/10.1016/j.sajb.2021.02.002

Mahmud JAL, Hasanuzzaman M, Nahar K, Rahman A, Hossain MS, Fujita M (2017) γ-aminobutyric acid (GABA) confers chromium stress tolerance in *Brassica juncea* L. by modulating the antioxidant defense and glyoxalase systems. Ecotoxicology 26 (5):675–690. https://doi.org/10.1007/s10646-017-1800-9

Millaleo R, Reyes-Díaz M, Alberdi M, Ivanov AG, Krol M, Hüner NPA (2013) Excess manganese differentially inhibits photosystem I versus II in Arabidopsis thaliana. J Exp Bot 64(1):343–354

Mishra RK, Mishra G, Singh R, Parihar P, Kumar J, Srivastava PK, Prasad SM (2022) Managing arsenic (V) toxicity by phosphate supplementation in rice seedlings: modulations in AsA-GSH cycle and other antioxidant enzymes. Environ Sci Pollut Res 29(10):14418–14429

Mita S, Murano N, Akaike M, Nakamura K (1997) Mutants of *Arabidopsis thaliana* with pleiotropic effects on the expression of the gene for β-amylase and on the accumulation of anthocyanin that are inducible by sugars. Plant J 11(4):841–851

Mostofa MG Fujita M (2013) Salicylic acid alleviates copper toxicity in rice (*Oryza sativa* L.) seedlings by up-regulating antioxidative and glyoxalase systems. Ecotoxicology 22 (6):959–973. https://doi.org/10.1007/s10646-013-1073-x

Mukta RH, Khatun MR, Nazmul Huda AKM (2019) Calcium induces phytochelatin accumulation to cope with chromium toxicity in rice (*Oryza sativa* L.). J Plant Interact 14 (1):295–302. https://doi.org/10.1080/17429145.2019.1629034

Nahar K, Hasanuzzaman M, Alam MM, Rahman A, Suzuki T, Fujita M (2016) Polyamine and nitric oxide crosstalk: Antagonistic effects on cadmium toxicity in mung bean plants through upregulating the metal detoxification, antioxidant defense and methylglyoxal detoxification systems. Ecotoxicol Environ Saf 126:245–255. https://doi.org/10.1016/j.ecoenv.2015.12.026

Najeeb U, Xu L, Ali S, Jilani G, Gong HJ, Shen WQ, Zhou WJ (2009) Citric acid enhances the phytoextraction of manganese and plant growth by alleviating the ultrastructural damages in *Juncus effusus* L. J Hazard Mater 170(2):1156–1163. https://doi.org/10.1016/j.jhazmat.2009.05.084

Nakano Y, Asada K (1981) Hydrogen peroxide is scavenged by ascorbate-specific peroxidase in spinach chloroplasts. Plant Cell Physiol 22(5):867–880

Nashef AS, Osuga DT, Feeney RE (1977) Determination of hydrogen sulfide with 5, 5′-dithiobis-(2-nitrobenzoic acid), N-ethylmaleimide, and parachloromercuribenzoate. Anal Biochem 79(1–2):394–405

Nelson N (1944) A photometric adaptation of the Somogyi method for the determination of glucose. J Biol Chem 153(2):375–380

Noor I, Sohail H, Hasanuzzaman M, Hussain S, Li G, Liu J (2022) Phosphorus confers tolerance against manganese toxicity in *Prunus persica* by reducing oxidative stress and improving chloroplast ultrastructure. Chemosphere 291:132999. https://doi.org/10.1016/j.chemosphere.2021.132999

Okant M, Kaya C (2019) The role of endogenous nitric oxide in melatonin-improved tolerance to lead toxicity in maize plants. Environ Sci Pollut Res 26(12):11864–11874. https://doi.org/10.1007/s11356-019-04517-3

Papadakis IE, Giannakoula A, Therios IN, Bosabalidis AM, Moustakas M, Nastou A (2007) Mn-induced changes in leaf structure and chloroplast ultrastructure of *Citrus volkameriana* (L.) plants. J Plant Physiol 164 (1):100–103. https://doi.org/10.1016/j.jplph.2006.04.011

Parashar A, Yusuf M, Fariduddin Q, Ahmad A (2014) Salicylic acid enhances antioxidant system in *Brassica juncea* grown under different levels of manganese. Int J Biol Macromol 70:551–558. https://doi.org/10.1016/j.ijbiomac.2014.07.014

Parvin K, Hasanuzzaman M, Mohsin SM, Nahar K, Fujita M (2021) Coumarin improves tomato plant tolerance to salinity by enhancing antioxidant defence, glyoxalase system and ion homeostasis. Plant Biol 23(S1):181–192. https://doi.org/10.1111/plb.13208

Polle A, Otter T, Seifert F (1994) Apoplastic peroxidases and lignification in needles of Norway spruce (*Picea abies* L.). Plant Physiol 106 (1):53–60

Principato GB, Rosi G, Talesa V, Giovanni E, Uotila L (1987) Purification and characterization of two forms of glyoxalase II from the liver and brain of Wistar rats. Biochim Biophys Acta (BBA)-Protein Struct Mol Enzymol 911 (3):349–355

Qureshi FF, Ashraf MA, Rasheed R, Ali S, Hussain I, Ahmed A, Iqbal M (2020) Organic chelates decrease phytotoxic effects and enhance chromium uptake by regulating chromium-speciation in castor bean (*Ricinus communis* L.). Sci Total Environ 716:137061. https://doi.org/10.1016/j.scitotenv.2020.137061

Rahman A, Hossain MS, Mahmud J-A, Nahar K, Hasanuzzaman M, Fujita M (2016) Manganese-induced salt stress tolerance in rice seedlings: regulation of ion homeostasis, antioxidant defense and glyoxalase systems. Physiol Mol Biol Plants 22(3):291–306. https://doi.org/10.1007/s12298-016-0371-1

Rasheed R, Arslan Ashraf M, Kamran S, Iqbal M, Hussain I (2018) Menadione sodium bisulphite mediated growth, secondary metabolism, nutrient uptake and oxidative defense in okra (*Abelmoschus esculentus* Moench) under cadmium stress. J Hazard Mater 360:604–614. https://doi.org/10.1016/j.jhazmat.2018.08.043

Rojas-Lillo Y, Alberdi M, Acevedo P, Inostroza-Blancheteau C, Rengel Z, MdlL M, Reyes-Díaz M (2014) Manganese toxicity and UV-B radiation differentially influence the physiology and biochemistry of highbush blueberry (*Vaccinium corymbosum*) cultivars. Funct Plant Biol 41(2):156–167. https://doi.org/10.1071/FP12393

Sahin S, Kısa D, Göksu F, Geboloğlu N (2017) Effects of boron applications on the physiology and yield of lettuce. Annu Res Rev Biol 21(6):1–7. https://doi.org/10.9734/ARRB/2017/38772

Saleh AM, Madany MMY, González L (2015) The Effect of Coumarin Application on Early Growth and Some Physiological Parameters in Faba Bean (*Vicia faba* L.). J Plant Growth Regul 34 (2):233–241. https://doi.org/10.1007/s00344-014-9459-4

Santos EF, Kondo Santini JM, Paixão AP, Júnior EF, Lavres J, Campos M, Reis ARd (2017) Physiological highlights of manganese toxicity symptoms in soybean plants: Mn toxicity responses. Plant Physiol Biochem 113:6–19. https://doi.org/10.1016/j.plaphy.2017.01.022

Sarker U, Oba S (2018) Response of nutrients, minerals, antioxidant leaf pigments, vitamins, polyphenol, flavonoid and antioxidant activity in selected vegetable amaranth under four soil water content. Food Chem 252:72–83. https://doi.org/10.1016/j.foodchem.2018.01.097

Sheng H, Zeng J, Liu Y, Wang X, Wang Y, Kang H, Fan X, Sha L, Zhang H, Zhou Y (2016) Sulfur mediated alleviation of mn toxicity in polish wheat relates to regulating mn allocation and improving antioxidant system. Front Plant Sci 7:1382. https://doi.org/10.3389/fpls.2016.01382

Skórka M, Sieprawska A, Telk A (2022) The implication of manganese surplus on plant cell homeostasis: A Review. J Plant Growth Regul 1–15

Socha AL, Guerinot ML (2014) Mn-euvering manganese: the role of transporter gene family members in manganese uptake and mobilization in plants. Front Plant Sci 5:106. https://doi.org/10.3389/fpls.2014.00106

Tripathi DK, Singh VP, Kumar D, Chauhan DK (2012) Impact of exogenous silicon addition on chromium uptake, growth, mineral elements, oxidative stress, antioxidant capacity, and leaf and root structures in rice seedlings exposed to hexavalent chromium. Acta Physiol Plant 34(1):279–289. https://doi.org/10.1007/s11738-011-0826-5

Ulhassan Z, Gill RA, Huang H, Ali S, Mwamba TM, Ali B, Huang Q, Hamid Y, Khan AR, Wang J, Zhou W (2019) Selenium mitigates the chromium toxicity in *Brassicca napus* L. by ameliorating nutrients uptake, amino acids metabolism and antioxidant defense system. Plant Physiol Biochem 145:142–152. https://doi.org/10.1016/j.plaphy.2019.10.035

Valivand M, Amooaghaie R (2021) Sodium Hydrosulfide Modulates Membrane Integrity, Cation Homeostasis, and Accumulation of Phenolics and Osmolytes in Zucchini Under Nickel Stress. J Plant Growth Regul 40(1):313–328. https://doi.org/10.1007/s00344-020-10101-8

Velikova V, Yordanov I, Edreva A (2000) Oxidative stress and some antioxidant systems in acid rain-treated bean plants: protective role of exogenous polyamines. Plant Sci 151(1):59–66

Wolfe K, Wu X, Liu RH (2003) Antioxidant activity of apple peels. J Agric Food Chem 51(3):609–614

Yang H, Shi G, Qiao X, Tian X (2011) Exogenous spermidine and spermine enhance cadmium tolerance of *Potamogeton malaianus*. Russ J Plant Physiol 58(4):622–628

Yang X, Han Y, Hao J, Qin X, Liu C, Fan S (2022) Exogenous spermidine enhances the photosynthesis and ultrastructure of lettuce seedlings under high-temperature stress. Sci Hortic 291:110570. https://doi.org/10.1016/j.scienta.2021.110570

Yemm EW, Willis AJ (1954) The estimation of carbohydrates in plant extracts by anthrone. The Biochem J 57(3):508–514. https://doi.org/10.1042/bj0570508

Yildiztugay E, Ozfidan-Konakci C, Karahan H, Kucukoduk M, Turkan I (2019) Ferulic acid confers tolerance against excess boron by regulating ROS levels and inducing antioxidant system in wheat leaves (Triticum aestivum). Environ Exp Bot 161:193–202. https://doi.org/10.1016/j.envexpbot.2018.10.029

Zhishen J, Mengcheng T, Jianming W (1999) The determination of flavonoid contents in mulberry and their scavenging effects on superoxide radicals. Food Chem 64(4):555–559

Zhou B, Guo Z, Xing J, Huang B (2005) Nitric oxide is involved in abscisic acid-induced antioxidant activities in *Stylosanthes guianensis*. J Exp Bot 56(422):3223–3228

Zhou J, Chen LH, Peng L, Luo S, Zeng QR (2020) Phytoremediation of heavy metals under an oil crop rotation and treatment of biochar from contaminated biomass for safe use. Chemosphere 247:125856. https://doi.org/10.1016/j.chemosphere.2020.125856